FLIGHT SAFETY FOUNDATION

OCTOBER 1994

# FLIGHT SAFETY
D I G E S T

# Flight Test of Takeoff Performance Monitoring System Indicates Successful Use in Research Vehicle

# Flight Safety Digest

**Vol. 13 No. 10** **October 1994**

## *In This Issue*



*Flight Safety Foundation is an international membership organization dedicated to improving aviation safety. Nonprofit and independent, the Foundation was launched in 1945 in response to the aviation industry's need for a neutral clearinghouse to disseminate objective safety information, and for a credible and knowledgeable body that would identify threats to safety, analyze the problems and recommend practical solutions to them. Since its beginning, the Foundation has acted in the public interest to produce a positive influence on aviation safety. Today, the Foundation provides leadership to nearly 600 member organizations in 75 countries.*

# Flight Test of Takeoff Performance Monitoring System Indicates Successful Use in Research Vehicle

***Computer system generates visual display that can help pilots monitor takeoff and make takeoff/abort decisions. Software can be adapted to modern airliners that are equipped with digital flight-control computers.***

*David B. Middleton*
*U.S. National Aeronautics and Space Administration*
*Langley Research Center*

*Raghavachari Srivatsan*
*ViGYAN Inc., Hampton, Virginia, U.S.*

*Lee H. Person Jr.*
*U.S. National Aeronautics and Space Administration*
*Langley Research Center*

In recent years, airplane safety has shown improvement in all segments of flight except during takeoff or abort situations. More than 4,000 takeoff-related accidents occurred between 1983 and 1990, resulting in 1,378 fatalities, according to the U.S. National Transportation Safety Board (NTSB). Among large airliners, 8.7 percent of all accidents occurred during takeoff or abort situations; for regional airliners, 12.5 percent occurred during this critical phase.[1]

Current flight management systems do not comprehensively or effectively monitor airplane performance on the runway. In particular, they do not provide pilots with timely knowledge of their measured along-track acceleration relative to a computed nominal acceleration based on existing conditions and standard (i.e., ideal) execution of the takeoff roll maneuver. They also do not provide explicit advisory "GO/NO-GO" decision aids during the takeoff roll.[2] Thus, many serious takeoff-related accidents might be prevented or downgraded to relatively safe, low-speed aborted takeoffs if an appropriate takeoff performance monitoring system were available to the flight crew.

Several performance monitoring systems and procedures of varying complexity have been proposed over the years, but none have been implemented and tested on commercial transport aircraft.[3–6] The U.S. National Aeronautics and Space Administration (NASA) Takeoff Performance Monitoring System (TOPMS) was developed as a computer software and hardware graphics system to assist pilots in the continual assessment of the takeoff situation. The TOPMS software drives cockpit displays that graphically indicate takeoff performance relative to a reference performance, engine condition and a continually updated prediction of the runway position where the airplane can be braked to a stop if an aborted takeoff becomes necessary. It also provides explicit GO/NO-GO advice in the form of situation advisory flags (SAFs).

The TOPMS has been evaluated in several phases at the Langley Research Center, Virginia, U.S. After a detailed TOPMS algorithm was formulated and developed in batch simulations,[7,8] initial head-down display (HDD) graphics were implemented and evaluated on the Langley Transport Systems Research Vehicle (TSRV) real-time, fixed-base Boeing 737 simulator. The TSRV airplane used for flight tests of the TOPMS is a highly modified Boeing 737-100 containing the research flight deck (aft) inside the fuselage (Figure 1, page 3). Figure 2 (page 4) is a photograph of the interior of the research flight deck; the front cover shows a close-up of the primary display (PD) navigational and TOPMS display (Nav/TOPMS), and the navigation control and display unit (NCDU).

The TOPMS algorithm was programmed on the TSRV existing flight displays computer. The airplane high-speed digital autonomous terminal access communication (DATAC) system supplied the algorithm with measured data from the airplane sensors and delivered computed data to drive symbology on the airplane's electronic display screens. Three sources of acceleration signals were used during the test series. The airplane body-mounted accelerometers and a gimbaled inertial measuring unit (IMU) generated satisfactory TOPMS input signals. Partway through the TOPMS test series, a strap-down air data and inertial reference system (ADIRS) package replaced the IMU on the TSRV. The ADIRS along-track acceleration signal was so noisy that its use was discontinued after six test runs. (In postflight analysis, this signal was found to be inadequately filtered for use in the runway research operations.)

The initial TOPMS displays were evaluated for content, credibility and comprehensibility by 32 research pilots, U.S. Air Force pilots and professional civilian pilots. They found that the displays were easy to monitor and provided valuable safety, performance and advisory information currently unavailable in commercial cockpits. In addition, the pilots suggested minor changes to the HDD graphics and recommended development of a simplified TOPMS head-up display (HUD) to complement the HDD.[9] A second simulation study that followed incorporated a revised HDD in front of each pilot and a simplified HUD in front of the pilot flying during takeoff. Seventeen evaluation pilots in the second study (including eight pilots who participated in the first study) provided additional insight into the desirability and importance of particular display symbology and formats.[10] Subsequently, the HDD graphics were revised further and the TOPMS was implemented on the TSRV research flight deck for the flight tests discussed in this report.

The TOPMS flight tests focused on verifying that the TOPMS would operate satisfactorily in a typically noisy airplane operating environment using preexisting flight computers, sensors, data buses and displays. The TOPMS displays were available only to the pilot in the research flight deck (viz., the TOPMS pilot) and only the latest version of the HDD symbology was tested. The test plan focused on producing appropriate displays for monitoring a variety of test conditions. Although most of the data gathered were qualitative, some numerical data were obtained during six test situations.

**Table 1**
**Symbols Used in This Report**

| | |
|---|---|
| $A_n$ | curve-fit coefficients, n = 0,1,2,3 (equation (2)) |
| a | acceleration, ft./sec.2 (equations (1) and (2)) |
| D | drag, lb. |
| $d_a$ | takeoff-roll computed distance from measured acceleration, ft. |
| $d_{gs}$ | takeoff-roll computed distance from measured ground speed, ft. |
| $d_{lt}$ | takeoff-roll measured distance from radar laser tracker, ft. |
| $d_p$ | take-off roll predicted distance from nominal acceleration, ft. |
| L | lift, lb. |
| m | mass, slugs |
| n | counter, consecutive error band excursions, n = 5,8,10 |
| T | thrust, lb. |
| $V_1$ | critical engine safety CAS (decision speed), knots |
| $V_2$ | takeoff safety CAS (climbout speed), knots |
| $V_R$ | rotation CAS, knots |
| $V_T$ | true airspeed, knots |
| W | airplane gross weight, lb. |
| $\mu_r$ | coefficient of rolling friction |

Source: U.S. National Aeronautics and Space Administration, Langley Research Center

The flight tests demonstrated that TOPMS technology developed on the TSRV B-737 simulator had been successfully transferred to the TSRV. The TOPMS algorithm predicted runway distances with reasonable accuracy, and the displays depicted the various test conditions and GO/NO-GO advisories correctly. For example, in six normal takeoff runs, most of the pretakeoff-predicted and real-time computed distances to accelerate the airplane to takeoff speed agreed within approximately two airplane (TSRV) lengths. A ground-based laser radar tracker at the Wallops Flight Facility, Virginia, U.S. continually measured the TSRV

**Cutaway View of TSRV B-737-100**

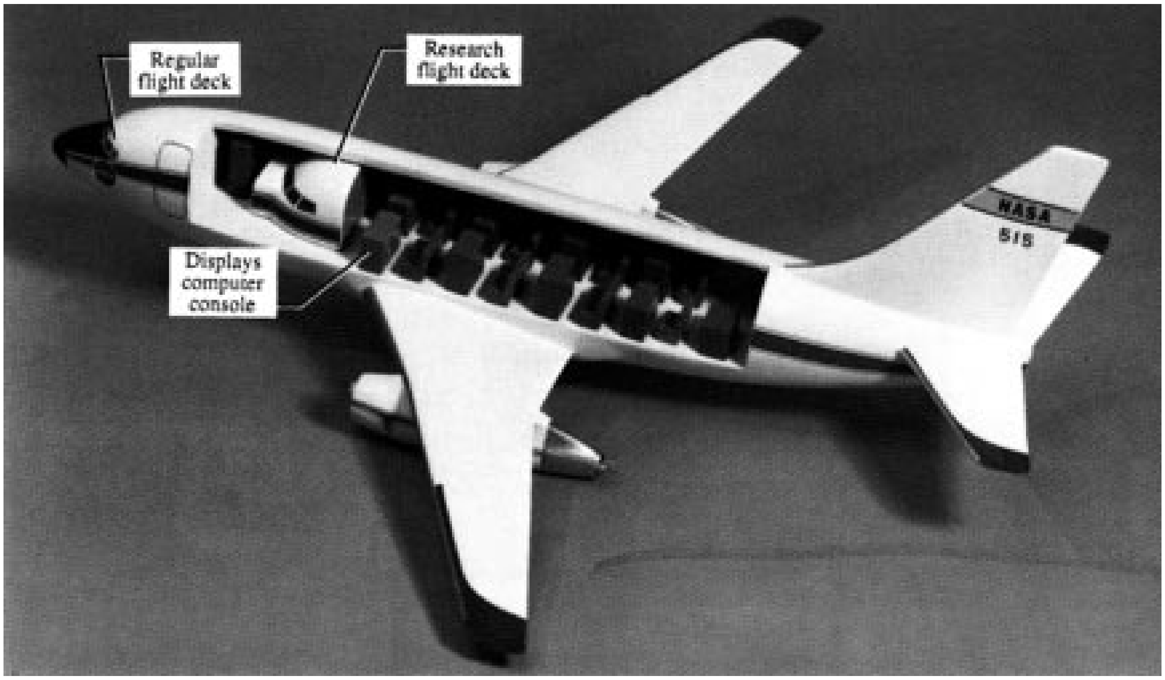


Source: U.S. National Aeronautics and Space Administration, Langley Research Center

**Figure 1**

range during two of these runs and showed that the airplane position when it reached rotation speed $V_R$ was approximately one half of an airplane length farther down the runway than was predicted during pretakeoff computations and approximately two lengths farther than the distance computed in real time by the algorithm. Similar agreement was obtained for two runs that were aborted at approximately 80 and 100 knots on dry pavement. Postflight analysis showed that had the airplane's independently measured ground speed been the basis of the computed runway distance in the two executed and two aborted takeoffs, the computed and measured distances would have been in much closer agreement.

The TOPMS is a computer software and hardware graphics system that visually displays engine status, runway performance and situation advisory information to aid pilots with their GO/NO-GO decision to continue or to abort a takeoff. The TOPMS algorithm computes and manipulates airplane performance and related data and commands the color display of both elemental and summary symbology. The elemental information consists of pretakeoff-predicted and real-time-measured indicators of performance and their effect on where the airplane is expected to reach takeoff speed or where it could be stopped in an abort situation (with maximum braking, but not reverse thrust). The summary information consists SAFs that alert and advise the pilots when the takeoff situation has degraded to the degree that it may be wise to abort — or not to abort if insufficient runway distance is available.

# Algorithm

The TOPMS algorithm consists of two segments: a pretakeoff segment and a real-time segment (Figure 3, page 6). The algorithm is briefly described in the next two sections; a detailed description of its development is given in references 7 and 8.

*Pretakeoff calculations.* When activated during pretakeoff, the algorithm obtains and uses nominal and/or current values for several key parameters (Table 2, page 5); checks for system anomalies such as misconfigured flaps or inconsistent input data; and determines scheduled values for engine pressure ratio (EPR), critical engine safety speed ($V_1$, also called decision speed), rotation speed ($V_R$) and takeoff safety speed ($V_2$). The algorithm extracts values for these parameters from data files that contain pertinent tables from the airplane flight manual.

Using data from detailed mathematical models of the engines, landing gear and aerodynamics for the host airplane, nominal values for the parameters listed in Table 2 and the appropriate EPR value for existing conditions, the algorithm calculates a predicted nominal acceleration performance of the airplane for the planned takeoff. It also predicts where $V_1$ and $V_R$ should occur during a nominal takeoff roll and warns the pilot when the length of the assigned runway appears too short for the planned takeoff.

The nominal performance is represented by a curve of nominal acceleration vs. true airspeed ($V_T$) generated from equations

**TSRV Research Flight Deck**

Source: U.S. National Aeronautics and Space Administration, Langley Research Center

**Figure 2**

1 and 2 and plotted with an appropriate curve-fitting method. Equation 1 defines the nominal acceleration during the takeoff roll as

$$a = \frac{T-D-\mu_r(W-L)\ m}{m} \qquad (1)$$

where the airplane approximate gross weight (W) is known, the rolling-friction coefficient ($\mu_r$) is estimated for the perceived runway surface condition, the values of lift (L) and drag (D) are obtained by the algorithm from the aerodynamics mathematical model, and thrust (T) is computed from the engine model for a typical throttle-movement history from idle to the position of scheduled EPR.

The same acceleration as a cubic polynomial in $V_T$ that is fitted to the equation 1 curve through the coefficients $A_n$ of the powers of $V_T$ (where n = 0,1, 2, 3) is expressed as

$$a = A_0+A_1V_T+A_2V^2{}_T+A_3V^3{}_T \qquad (2)$$

The conversion process involves the following steps:

1. Equation 1 is solved using an extremely low value of $\mu_r$ = 0.005 and nominal values for other conditions over the takeoff speed range. The resulting curve (after engine spool-up transients settle out) is plotted as the upper boundary in Figure 4 (page 6) over a speed range from approximately 10 knots to $V_R$ speed.

2. Equation 1 is solved again for an extremely high value of $\mu_r$ = 0.04 and plotted as the lower boundary in Figure 4 over the same speed range.

3. Equation 2 is fitted to each of the above curves using the sum of least-squares error method. As shown in Figure 4, the correlation using this method is excellent (the computed and fitted curves for each value of $\mu_r$ essentially lie on top of each other).

4. The two sets of curve-fit coefficients are then stored where the algorithm can access them when subsequently creating a nominal acceleration curve corresponding to any estimated value of $\mu_r$ = 0.005 to 0.040.

A representative nominal acceleration curve for a dry surface ($\mu_r$ = 0.015) is plotted as a solid line in Figure 5 (page 7). This curve is created by linear interpolation of the two sets of curve-fit coefficients obtained above. After the curve-fitting process is complete, the pretakeoff segment nominal performance parameters are transferred to the real-time segment, as shown in Figure 3 (page 6). This process is treated in considerable detail in reference 8.

*Real-time calculations.* A block diagram portraying real-time operations is shown in Figure 6 (page 8).

The functions performed by most of the blocks are self-explanatory; the measured inputs enter from the left and the computer-estimated outputs emerge at the right. At low speeds, the algorithm uses measured ground speed and wind to compute airspeed; then at approximately 40 knots, the airplane real-time-computed airspeed becomes valid and replaces airspeed derived from integrated ground speed by means of the software switch shown at the left center of Figure 6. During the test runs, airplane positions on the runway were determined from distances traveled calculated by double integration of measured accelerations (method 1). During postflight analysis (only), single integration of the independently measured ground speed provided another means of determining airplane position (method 2 is shown by the dashed line at the top of Figure 6).

The real-time segment of the algorithm is activated when the pilot advances the throttles forward from idle. As the airplane rolls down the runway, the distance traveled and the distances required to reach $V_1$ and $V_R$ are continually computed using sensor-measured values for the parameters shown in Table 3 (page 7).

The algorithm also creates a reference acceleration curve in real time in the following manner:

1. While the throttles are being advanced and/or adjusted, a reference acceleration is computed from equation 1 using thrust values associated with the sensed EPR and otherwise nominal input data.

2. As soon as the throttles are set (i.e., become stationary for more than three seconds), the algorithm makes a one-time $\mu_r$ adjustment to the reference acceleration curve by forcing the reference acceleration value at a given true airspeed to match that of the measured acceleration. This adjustment is achieved by appropriately changing the value of $A_0$ in equation 2.

3. The algorithm also makes a one-time adjustment to the along-track component of the wind. After the calibrated airspeed (CAS) measurement becomes valid, an along-track component of the wind is calculated from measured ground speed and CAS; this value is then substituted for the initial value for the remainder of the takeoff.

**Table 2**
**Pretakeoff Inputs to TOPMS Algorithm**

| |
|---|
| Airplane center of gravity |
| Airplane gross weight |
| Airplane flap setting |
| Pressure altitude |
| Wind direction |
| Wind speed |
| Ambient temperature |
| Runway rolling friction coefficient |

Source: U.S. National Aeronautics and Space Administration, Langley Research Center

As indicated above, the $\mu_r$- and wind-error adjustments are programmed to execute only once per run. Nevertheless, each time the throttles are moved appreciably, the algorithm adjusts the reference acceleration curve according to the EPR levels it associates with each newly measured throttle position.

Throttle movements and settings that differ from those assumed when the nominal acceleration curve was created are not treated by the TOPMS algorithm as error conditions; instead, they produce a reference acceleration curve that is parallel to the nominal acceleration curve. In particular, during a low throttle takeoff, the displays will not indicate an engine problem and SAFs will not appear if the remaining runway distance will accommodate the extended takeoff. The algorithm could be rewritten to treat off-nominal throttle settings as an error; but because such an error is easily corrected by moving the throttles, low-throttle settings probably should not be included in the abort criteria.

The algorithm real-time segment continually computes the difference between measured acceleration and reference acceleration. If the magnitude of the resulting error signal exceeds a specified level, an abort SAF is displayed.

The front cover shows a close-up of the displays in the TSRV aft research flight deck. The upper primary display (PD) screen provides attitude, altitude and speed information. The existing PD system configuration was used without modification for the TOPMS tests. The navigation display (ND) in the center of the photograph presents either TOPMS information while the airplane is on the ground or regular navigational information after the airplane becomes airborne. The keypad on the unit below the ND screen is used to enter data into the airplane computers.

The TOPMS display consists of a runway graphic with passive and active symbology on and around it. Figure 7

## Functions of the TOPMS Algorithm

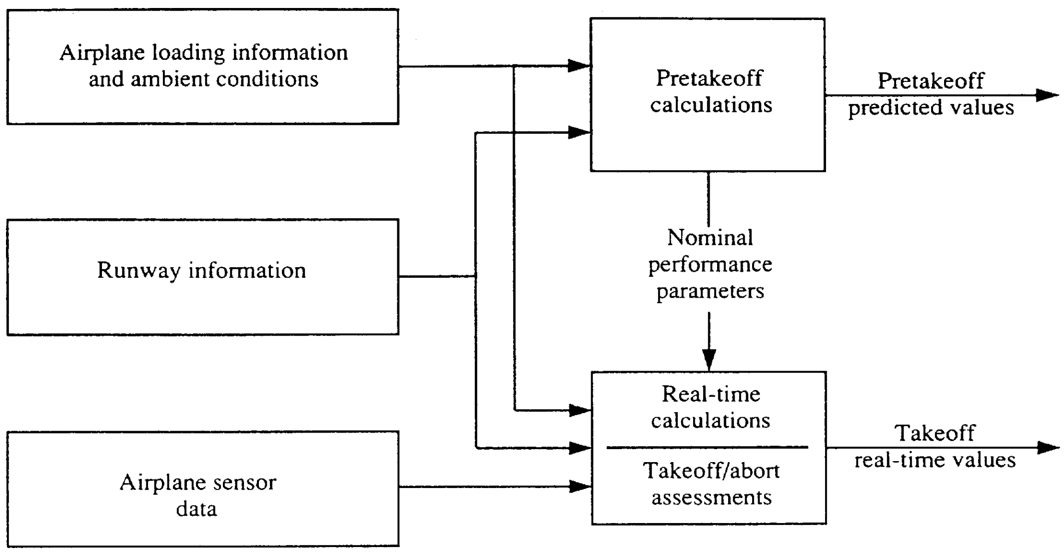


Source: U.S. National Aeronautics and Space Administration, Langley Research Center

**Figure 3**

(page 9) illustrates the display for two situations: the takeoff-roll display (Figure 7(a)) shows a takeoff roll underway in which acceleration performance has become unsatisfactory and an abort is being advised. The abort display (Figure 7(b)) shows a takeoff roll in which an abort has been initiated and partial braking is underway.

The takeoff-roll situation illustrated in Figure 7(a) shows the airplane about halfway down a 6,000-foot (1,829-meter) runway traveling at a CAS of 97 knots (displayed in the box left of the airplane symbol). Pretakeoff computations for this case were based on nominal acceleration and the algorithm predicted that a decision speed $V_1$ of 126 knots and a rotation speed $V_R$ of 128 knots could be achieved near the unshaded triangle. Nevertheless, during the takeoff roll, actual acceleration was considerably below nominal, which caused the horizontal $V_1$ and $V_R$ lines and caused the shaded triangle to move forward. Specifically, the position of the $V_R$ line corresponds to the computed along-track position of the shaded triangle apex. This forward movement of the shaded triangle is an indirect but an important indication of the acceleration deficiency.

## Acceleration Curves for Extreme Values of $\mu_r$

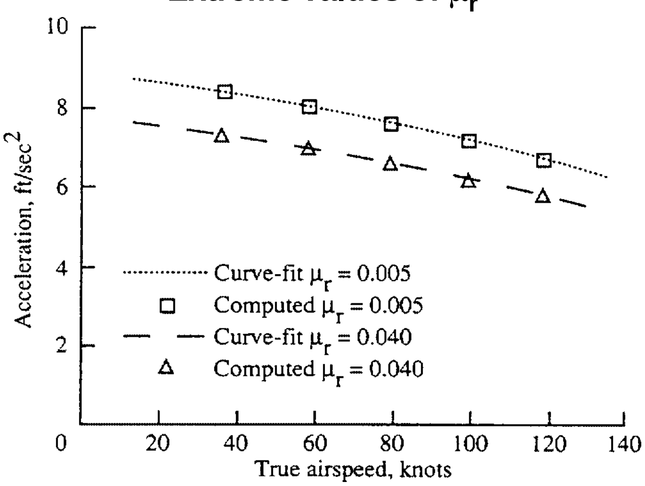


Source: U.S. National Aeronautics and Space Administration, Langley Research Center

**Figure 4**

The algorithm initially determines whether a U.S. Federal Aviation Administration (FAA)-sanctioned takeoff[11] can be expected; it computes whether the airplane can achieve $V_R$ before it reaches the ground-roll limit line (GRLL). The GRLL marks the farthest downfield position where the airplane, after undergoing a critical engine failure at $V_1$, can initiate rotation and barely clear a 35-foot (11-meter) barrier at the end of the runway. The minimum takeoff field length is the total distance required to reach $V_R$ plus the ground and air distance beyond $V_R$ for completing the takeoff described above.

For the situation illustrated in Figure 7(a) the ground and air distance beyond $V_R$ is subtracted from total runway length (6,000 feet [1,829-meters]) to establish the location of the GRLL. Note that a takeoff-roll safety margin of approximately 500 feet (152 meters) is evident between the apex of the shaded triangle (viz., the $V_R$ line) and the GRLL. The GRLL has no direct relationship to the bottom of the

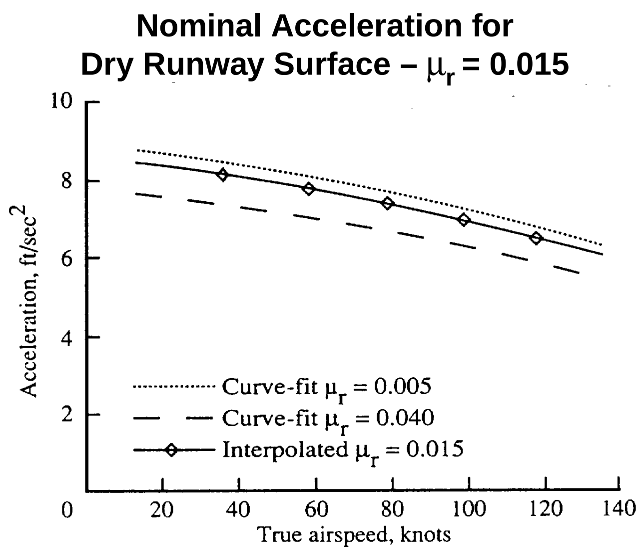


Source: U.S. National Aeronautics and Space Administration, Langley Research Center

**Figure 5**

EPR bars; they were arbitrarily based at the GRLL on the display format.

In the off-nominal situation depicted in Figure 7(a), both engines appear to be operating normally. The EPR bars are extended up to the target level, but the shaded triangle and the $V_1$ and $V_R$ lines have moved noticeably forward from their nominal locations depicted by the unshaded triangle. The algorithm has determined that an abort may be the most appropriate control action for this situation and the display conveys this advice to the pilot by means of the STOP SAF that appears at the end of the runway graphic. At the same time, an x appears just beyond the GRLL and shows where the airplane will come to a stop with maximum application of the wheel brakes and full deployment of the spoilers (i.e., speed brakes). Normally, the x remains hidden until the computed stop point is beyond the GRLL; when an abort is advised, the x is unmasked simultaneously d with the appearance of the STOP sign. The benefit of using reverse thrust is not included in the calculation of the x position; however, reverse thrust can be used to advantage in situations where both engines appear to be working satisfactorily.

Figure 7(b) shows the TOPMS display after an abort has been initiated. All takeoff-related information has been removed from the runway graphic except the airplane symbol, which shows position on the runway; ground speed, which replaces CAS in the speed box; and the x, which locates the maximum-braking stop point. An additional symbol, shaped like a football, has appeared that denotes the predicted stop point based on the measured acceleration. Less than maximum braking is required whenever the football position is ahead of the x.

A summary of SAF responses based on sensor data during various flight situations is shown in Table 4 (page 8). (The absence of an SAF indicates that the takeoff is proceeding normally and/or airplane parameters are staying within acceptable error bands.) For example, the SAF indicating flight situation 4 informs the pilot at a critical high-speed point that an engine has failed and that adequate runway distance remains to stop the airplane if the GO option suddenly becomes unreasonable (e.g., when smoke is rapidly engulfing the cabin).

No still photographs of the displays were made during actual flight tests. Instead, all photographs except those in Figure 1, Figure 2 (page 4) and the front cover, were recreated in a Langley special-purpose test facility, the Experimental Avionics System Integration Laboratory (EASILY). In essence, EASILY is a hot-bench extension of the flight test bed. It contains duplicates of the actual flight hardware and software along with a high-fidelity, nonlinear computer model of the Boeing 737-100 — the same model as the TRSV used during the TOPMS simulation studies.[9,10]

## Pretakeoff Displays

If the flap positions do not agree with the nominal position specified for the pretakeoff calculations, the partially generated TOPMS display shown in Figure 8 (page 10) will appear on the screen. No additional TOPMS graphics are generated until the flap lever is put in the proper detent and the flaps move to the commanded position.

If the length of the assigned runway is shorter than the minimum distance determined by the algorithm, a TOPMS display similar to the one in Figure 9 (page 10) will appear. Note that the apex of the $V_R$ triangle is well beyond the GRLL (horizontal line across the runway symbol), which causes a STOP sign to appear that advises the pilot not to start the takeoff roll.

If the runway is long enough, the flaps are correctly set and the conditions are otherwise normal, a fully generated pretakeoff TOPMS display similar to the graphic shown in Figure 10 (page 11) will appear. This graphic shows where $V_1$

**Table 3**
**Additional Real-time Inputs To TOPMS Algorithm**

| |
|---|
| Left and right engine pressure ratios |
| Left and right throttle positions |
| Airplane flap settings |
| Airplane accelerations |
| Airplane ground airspeed |
| Calibrated airspeed |

Source: U.S. National Aeronautics and Space Administration, Langley Research Center

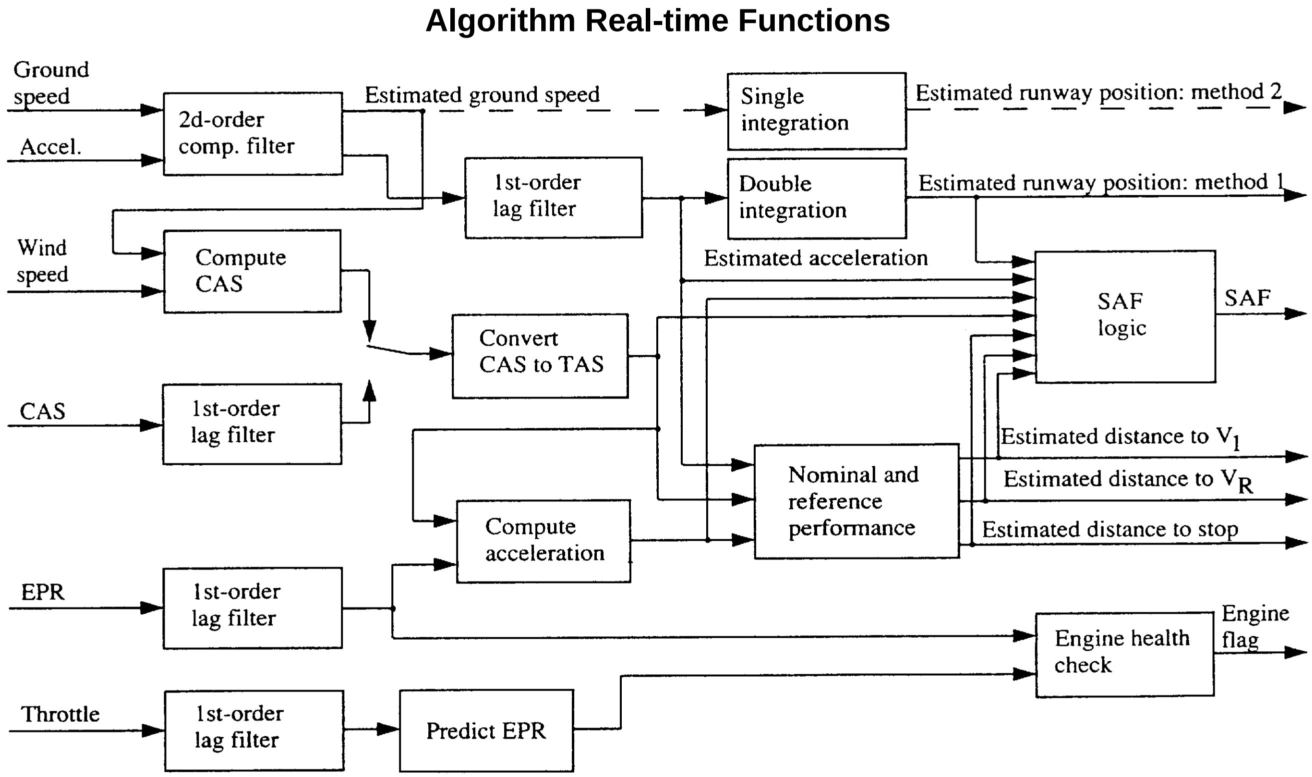


Source: U.S. National Aeronautics and Space Administration, Langley Research Center

**Figure 6**

of 122 knots and $V_R$ of 124 knots should occur with respect to the airplane's initial position on the runway. (For viewing clarity, the computed airplane position is depicted by the nose of the airplane graphic.) The length of the assigned runway (6,000 feet [1,829-meters]) and the point where the takeoff roll will start have been entered; the algorithm has scaled the corresponding runway graphic to span the entire usable vertical range of the display screen. At this stage, the TOPMS

**Table 4**
**Shapes, Colors and Conditions for Situational Advisory Flags**

| | | | | |
|---|---|---|---|---|
| [No flag] | | 1. | Takeoff roll proceeding satisfactorily. | GO |
| Rectangular | Green | 2. | No engines failed; airplane can attain $V_R$ before reaching GRLL but stopping on runway doubtful. | GO |
| | | 3. | One engine failed when CAS > $V_1$; airplane can attain $V_R$ before reaching GRLL or can easily stop on runway. | GO |
| Triangular | Amber (blinking) | 4. | One engine failed at CAS > $V_1$; airplane can attain $V_R$ well before reaching GRLL or can easily stop on the runway. | EITHER |
| Octagonal | Red | 5. | One engine failed at CAS < $V_1$. | NO-GO |
| | | 6. | Both engines failed. | NO-GO |
| | | 7. | Predicted rotation point beyond GRLL. | NO-GO |
| | | 8. | Measured along-track acceleration not within the specified error band about the reference acceleration. | NO-GO |

Source: U.S. National Aeronautics and Space Administration, Langley Research Center is ready for the takeoff roll to begin. (The zero-length EPR bars depicting idle thrust are not perceptible in Figure 10.)

## Takeoff-roll Displays

Photographs of representative displays for several flight situations are presented in Figures 11–18.

*Normal takeoff roll.* Figure 11 (page 11) shows a typical TOPMS display during a normal takeoff roll on a 6,000-foot runway. The airplane is traveling at a CAS of 83 knots. Note that the top ends of both EPR bars match their target levels (1.95) and that the $V_R$ triangles have not separated. Under such conditions, the pilot can expect to reach $V_R$ approximately halfway down the runway and the monitoring tasks would primarily be to keep track of airspeed and occasionally to glance at the $V_R$ triangle and EPR bars. The pilot can monitor airspeed by watching the numerals in the speed box or by observing the closure of the moving CAS line on the near-stationary $V_1$ line. The pilot can also keep the analog display of airspeed within peripheral vision range while continuing to focus on the real-world runway scene.

If an engine were to fail before the airplane reaches $V_1$ (during an otherwise normal takeoff situation), it would produce a head-down TOPMS display similar to the one shown on the front cover. In this instance, the right engine has failed at approximately 100 knots and the display is conveying an abort SAF (STOP sign) to the pilot. In addition, the algorithm has determined that for an immediate abort and use of maximum braking, the airplane can be stopped at the x shown about halfway down the 6,000-foot runway.

*Low-throttle takeoff roll.* Figure 12 (page 12) shows the TOPMS display for a situation in which the throttles were not advanced to the nominal position for attaining scheduled EPR (selected during pretakeoff by the algorithm from the database programmed from the TSRV flight manual). The

**TOPMS Takeoff-roll and Abort-display Symbology**

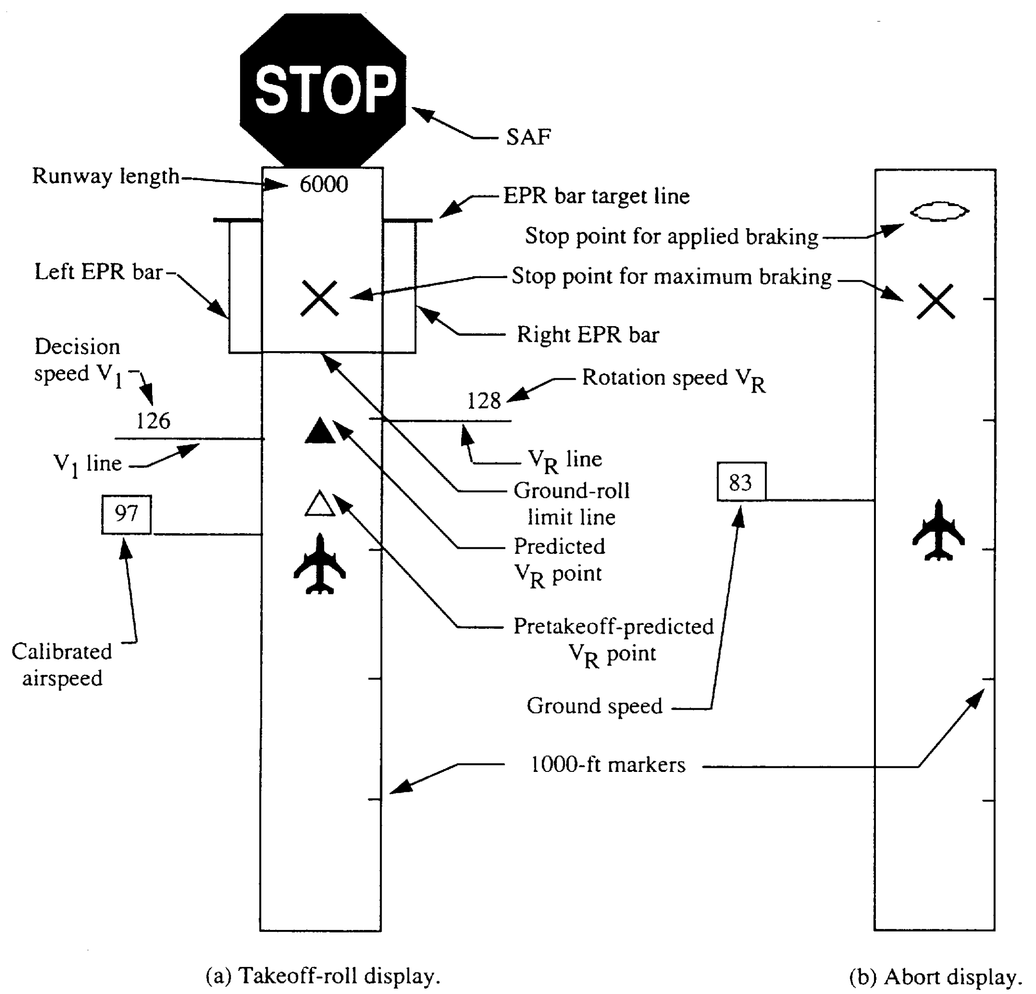


Source: U.S. National Aeronautics and Space Administration, Langley Research Center

**Figure 7**

## TOPMS Display with Flaps in Wrong Position

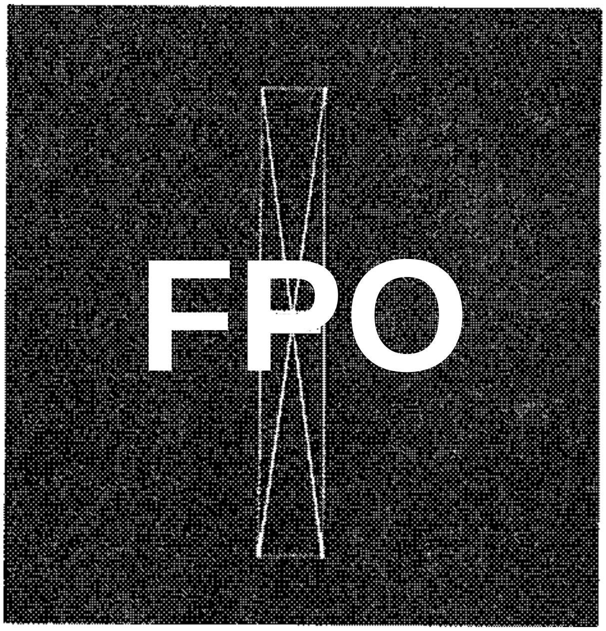


Source: U.S. National Aeronautics and Space Administration, Langley Research Center

**Figure 8**

shaded triangle has moved forward nearly 1,000 feet (305 meters) from its initial location where it had been superimposed on the unshaded triangle. If the shaded triangle remains stationary at this new position, it signifies that thrust is correct for the actual throttle setting and no acceleration error exists. The throttles can be advanced to reduce this separation or the takeoff roll can be continued at reduced thrust with the expectation of a satisfactory takeoff. In alternate form, the algorithm could respond to the low-throttle settings with error condition graphics; this was not the choice in any of the TOPMS studies.[7–10,12]

*Engine failure during low-throttle takeoff roll.* If an engine fails during a reduced-thrust takeoff-roll situation, the TOPMS display will be similar to the graphic shown in Figure 13 (page 12). An engine failure is declared by the algorithm when the engine EPR has degraded by more than a specified amount (10 percent in this study) from the value normally produced for the measured throttle position. For the situation in Figure 13, the under-advanced throttles are commanding both engines to produce EPRs of approximately 1.7 rather than the scheduled 1.95. The left engine is apparently producing the commanded EPR value of 1.7; however, the EPR bar for the failed right engine is clearly less than 90 percent of the length of the apparently correct left EPR bar and has turned red. Concurrently, a red SAF (STOP sign) and a predicted stop-point x have appeared and the $V_R$ triangles have separated by more than 1,000 feet (305 meters). If the performance of the faulty engine degrades further, the shaded triangle will continue to advance toward the GRLL. At this stage, takeoff is still a viable option; however, NO-GO is the control action recommended by the TOPMS before airplane speed increases further and the remaining runway distance becomes more marginal.

*Engine failure at high speed.* If an engine failure occurs near $V_1$ on a relatively short runway, as shown in Figure 14 (page 13), the SAF is displayed as a large green rectangle at the end of the runway graphic. This symbol advises the pilot that the best option is to continue with the takeoff because a maximum braking stop would likely terminate near or beyond the end of the runway pavement. (See the x in Figure 14.) Also, note in Figure 14 that the current CAS = 124 knots is greater than the decision speed $V_1$ = 120 knots, which is an overriding condition that warrants continuation of the takeoff.

If a similar situation were encountered on a very long runway, the TOPMS would exhibit a blinking triangular GO/NO-GO SAF like the one shown in Figure 15 (page 13). The blinking amber SAF signifies that an engine has failed at or above $V_1$ and that the two viable control options include continuing the takeoff as currently required by regulations[11] or undertaking a dangerous high-speed abort (e.g., in a perceived critical emergency such as fire or smoke in the cabin). For the situation in Figure 15, the predicted maximum-braking stop-point x is about 6,000 feet (1,829 meters) down the 10,000-foot (3,048-meter) runway.

## TOPMS Display When Assigned Runway Too Short

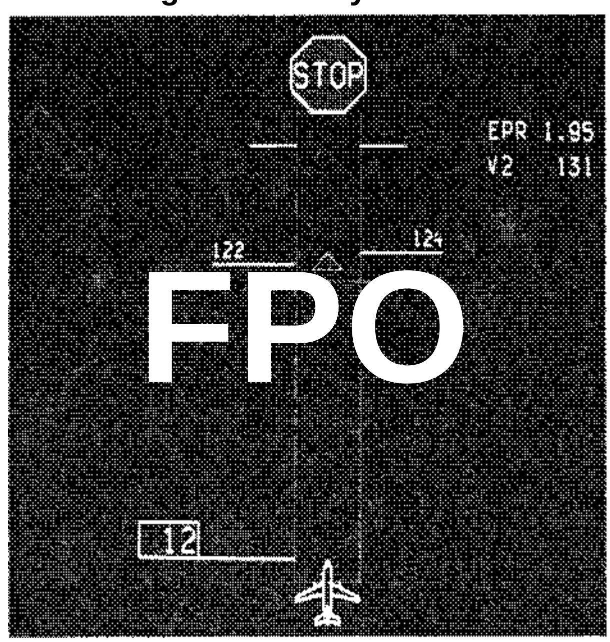


Source: U.S. National Aeronautics and Space Administration, Langley Research Center

**Figure 9**

*Excess drag vs. EPR sensor error.* Ascertaining whether excessive drag and/or large EPR sensor errors are causing significantly lower than nominal performance involves the following condition checks by the algorithm:

1. Engine performance is checked. A failing engine produces lower than scheduled EPR and a correspondingly lower acceleration level. When the EPR error for this engine becomes unacceptable (i.e., the measured EPR level differs by more than 10 percent from the EPR level associated with the measured throttle position), the algorithm changes the color of the shortened EPR bar to red and displays the appropriate SAF (see front cover). If the pilot chooses not to abort immediately, the algorithm will continue to provide information on the magnitude and trend of the acceleration deficiency by the position and movement of the shaded triangle and on the EPR condition of the unfailed engine by the length and color of its associated EPR bar.

2. If no engine has failed and the throttles have a lower than nominal setting (Figure 12, page 12), the EPR bars will accordingly stop short of their target mark, but they will not change color. The shaded triangle will also move noticeably forward; no SAF will be displayed unless the triangle moves beyond the GRLL.

**TOPMS Display When Ready to Begin Takeoff**

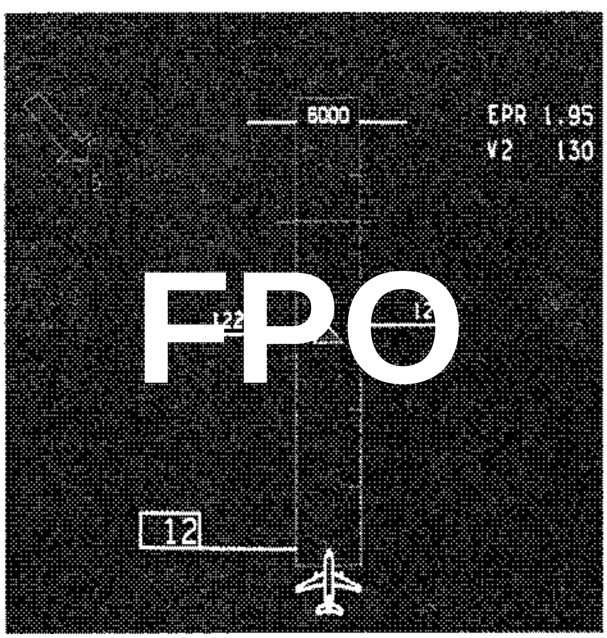


Source: U.S. National Aeronautics and Space Administration, Langley Research Center

**Figure 10**

**TOPMS Display when Normal Takeoff Under Way**

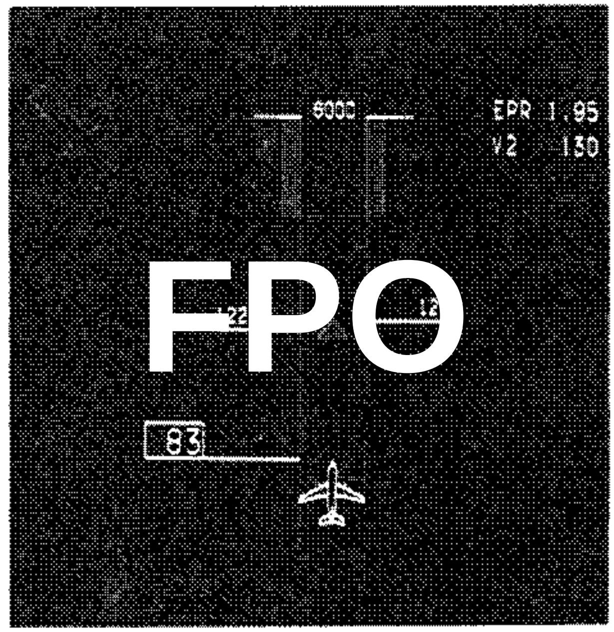


Source: U.S. National Aeronautics and Space Administration, Langley Research Center

**Figure 11**

3. If the EPR bars rise to and remain at their scheduled target level without changing color and the shaded triangle continually drifts forward, the indication is that drag is increasing faster than it should for the other conditions (e.g., wind, temperature and weight). The situation is illustrated in Figure 16 (page 13). When the incremental drag becomes excessive, causing the acceleration error to exceed the acceptable level of 10 percent, a red SAF (STOP sign) will appear as shown in Figure 17 (page 14). Nevertheless, if one or both EPR bars turn red while remaining at the target length, a serious EPR sensor error exists and a red SAF will appear as shown in Figure 18 (page 14). Note in this figure that the shaded triangle has also crossed the GRLL, thus satisfying another abort criterion (situation 7 in Table 4, page 8). (A relevant, real-world situation that resulted from an EPR sensor error is discussed later in this article.)

## Abort Displays

Figure 19 (page 15) shows photographs of abort displays for three situations. Each display contains two computer-predicted stop-point symbols — the x that is carried over from the takeoff display and the football-shaped symbol that appears on the runway graphic as soon as the brakes are applied. The football locates where the stop point will be, based on the currently computed position, speed and measured acceleration. The display in Figure 19(a) shows the football ahead of the x, which indicates that less than full braking is being applied. The display

**TOPMS Display with Throttle Set Lower Than Scheduled**

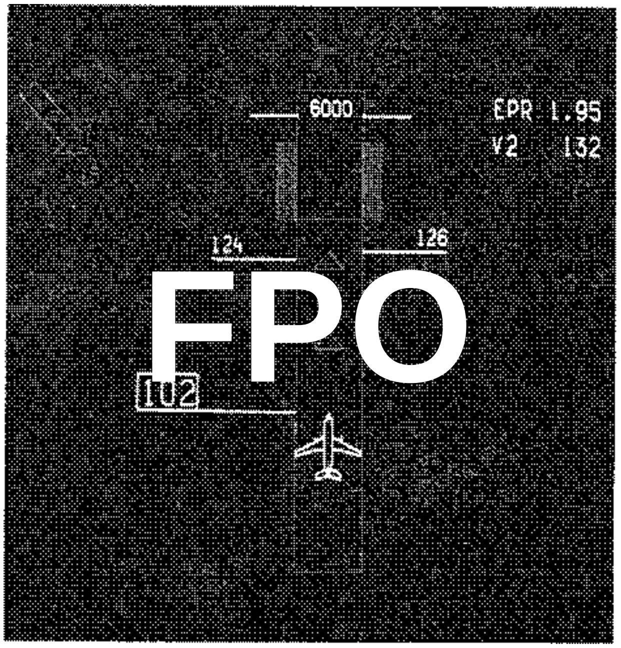


Source: U.S. National Aeronautics and Space Administration, Langley Research Center

**Figure 12**

**TOPMS Display for Engine Failure During Reduced-throttle Takeoff**

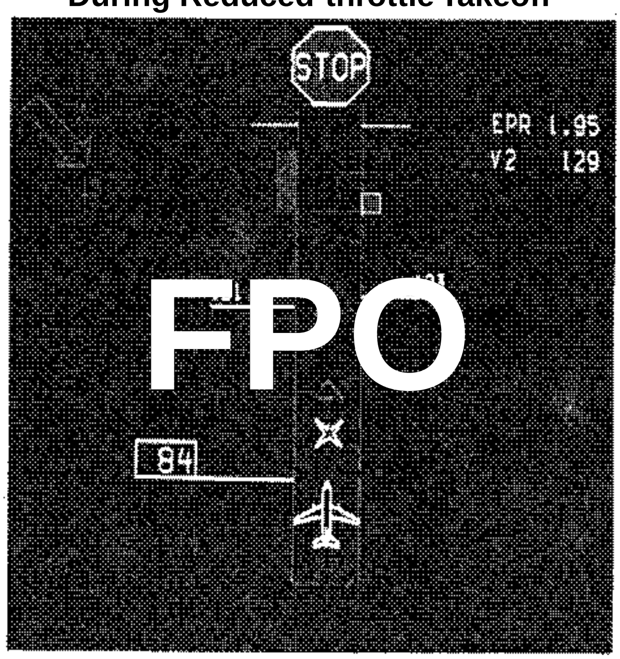


Source: U.S. National Aeronautics and Space Administration, Langley Research Center

**Figure 13**

in Figure 19(b) shows the football superimposed on the x, which indicates that full braking is being applied. The display in Figure 19(c) indicates that full braking and reverse thrust are being applied to stop the airplane slightly before the x is reached.

## Test Equipment

The TSRV is a production prototype Boeing 737-100 (Figure 1, page 3), and its fuselage is filled with numerous computers, recorders, data-transfer systems and the aft research flight deck, which permit the use and evaluation of advanced electronic displays and fly-by-wire controls. A TOPMS display was not provided in the TSRV forward regular flight deck; brake controls and HUD were not provided in the research flight deck. Because of these equipment limitations, the TOPMS was remotely tested in the HDD mode only.

A functional block diagram of the test hardware is shown in Figure 20 (page 16). Although the TOPMS pilot and TOPMS displays were located remotely, the procedures were set up to simulate a side-by-side, real-world piloting situation. The TOPMS pilot and the pilot flying communicated by intercom.

The TOPMS software was programmed on the Norden 11/70 displays computer console (Figure 1, page 3) along with the software for the other airplane displays. Except for a video camera and an additional remote display screen, no extra hardware had to be installed to document the real-time performance of the TOPMS displays under the various test situations. Research observations and conversations among the pilots, the flight director and the control tower were recorded on the audio channel of the videotapes.

The TOPMS interfaced with the flight decks, sensors and other experimental equipment through the airplane global digital autonomous terminal access communication (DATAC) data bus.[13] In addition, a ground-based FPS-16 Radar/Laser Tracker[14] at the Wallops Flight Facility was used to track the airplane during several of the test runs; it independently provided distance measurements as functions of time. Subsequently, these data were time-merged with the data recorded onboard the airplane, which permitted a comparison of measured and computed stop distances. Sixteen channels of strip-chart data were monitored during the test runs to verify in real time that a test run appeared to be proceeding properly. In addition, approximately 60 airplane and TOPMS parameters were digitally recorded at a rate of 20 samples per second for postflight scrutiny and analysis.

Six days of flight testing were conducted between March 1987 and November 1989 at the Wallops Flight Facility and the Langley Air Force Base in Virginia, the Kennedy Space Center Shuttle Landing Facility and the Patrick Air Force Base in Florida and the Asheville Regional Airport in North Carolina. The test runs included 55 takeoff and 30 abort situations. All were made on dry pavements ranging from

**TOPMS Display for Engine Failure Near $V_1$ on Short Runway**

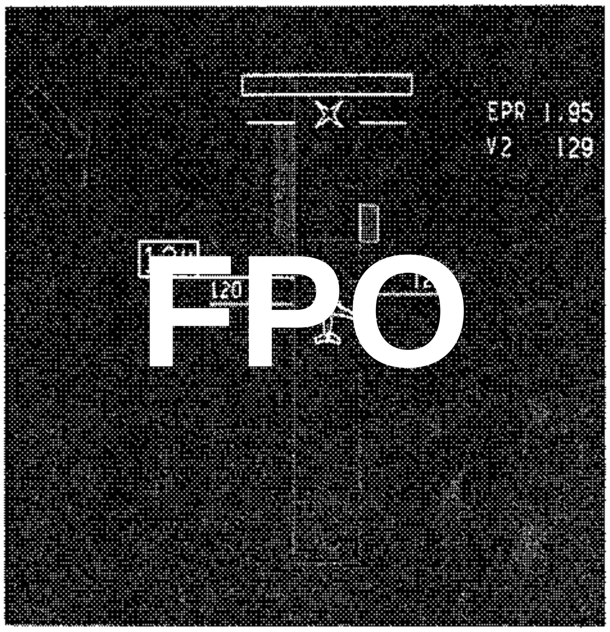


Source: U.S. National Aeronautics and Space Administration, Langley Research Center

**Figure 14**

slurry-sealed asphalt to highly grooved concrete. During the test series, temperatures ranged from approximately 25 degrees F to 85 degrees F (4 degrees C to 29 degrees C) and gross weights varied from heavy to light depending on the amount of fuel onboard.

## Flight-test Crew

As indicated in Figure 20 (page 16), the TOPMS flight-test crew consisted of a pilot flying who controlled the airplane from the left seat of the TSRV regular flight deck, a TOPMS pilot who monitored the TOPMS displays in the research flight deck and communicated with the pilot flying by the intercom and a safety pilot who occupied the right seat in the TSRV regular flight deck and participated minimally in the test program. (During a checkout flight, a four-inch [10-centimeter] monitor was temporarily mounted in the center console of the TSRV regular flight deck for the safety pilot to observe; however, it was too small to be useful and was removed before the actual test flights began.)

## Acceleration Measurements

Three airplane along-track acceleration signals were available, of which one was selected for input to the algorithm during the test, and two reference accelerations were generated by the algorithm. During pretakeoff, a nominal acceleration curve for $\mu_r = 0.015$ (Figure 5, page 7) was generated for initial

**TOPMS Display for Engine Failure After Reaching $V_1$ on Very Long Runway**

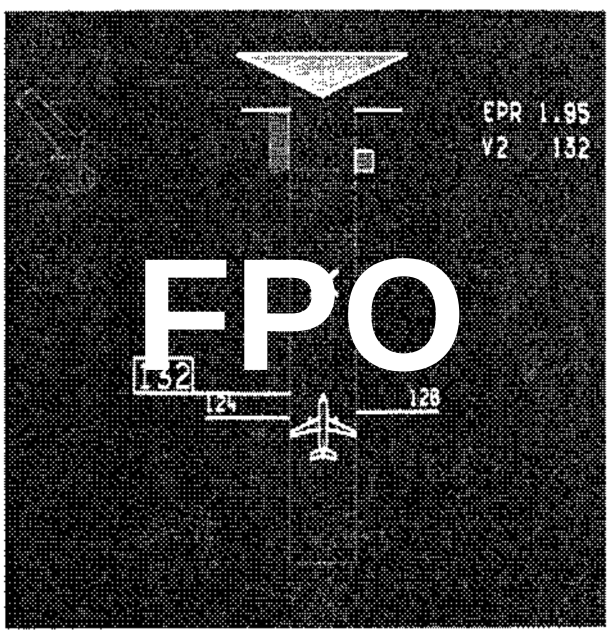


Source: U.S. National Aeronautics and Space Administration, Langley Research Center

**Figure 15**

**TOPMS Display with Acceptable Acceleration Deficiency**

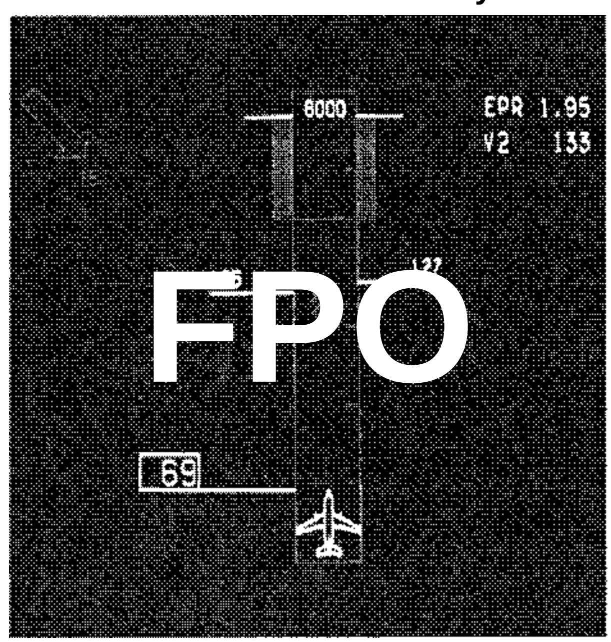


Source: U.S. National Aeronautics and Space Administration, Langley Research Center

**Figure 16**

**TOPMS Display with Unacceptable Acceleration Performance**

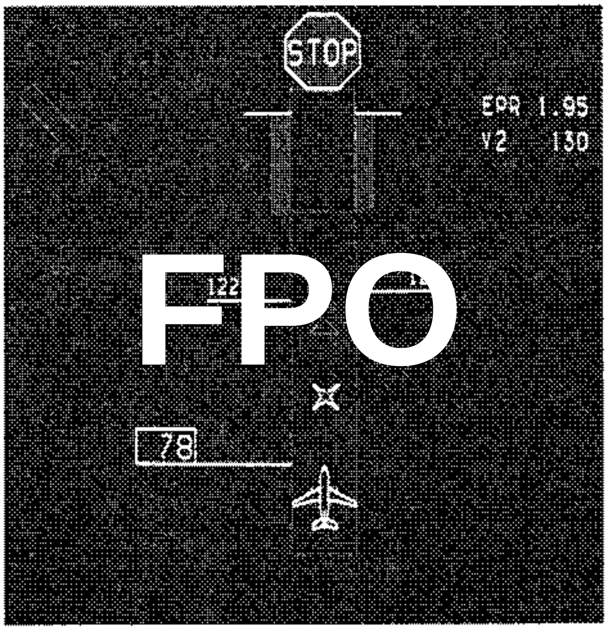


Source: U.S. National Aeronautics and Space Administration, Langley Research Center

**Figure 17**

predictions of where particular performance events would occur based on existing and/or expected conditions. Then, during the takeoff roll, a reference acceleration curve was generated to reflect input deviations such as higher- or lower-than-nominal throttle setting, wind and μr updates.

During the six days of testing, measured along-track acceleration signals were obtained from the airplane inertial measuring unit (IMU), which was available during the first three test days; an air data and inertial reference system (ADIRS), which replaced the IMU for part of the fourth test day; and the airplane body-mounted x-axis accelerometer, which was available for all test days but was used as a TOPMS input only during the last two and a half test days. Pitch compensation was appropriately added to each of the measured along-track acceleration signals to account for the 1 degree inclination of the TSRV body x-axis to the runway surface and to accommodate the takeoff rotation.

After a few runs on the fourth test day (Table 5, page 17), the ADIRS along-track acceleration signal was discarded in favor of the body-mounted x-axis acceleration signal. As is discussed later, the along-track acceleration signal from the TSRV ADIRS unit was found to be atypical of the high-quality, filtered acceleration signals available on modern airplanes.

Before the actual test runs, the TSRV was taxied at moderate speed down a runway at the Wallops Flight Facility while the safety pilot called off 1,000-feet- (305 meter-) to-go markers as the airplane physically passed them; the TOPMS pilot, having no outside view, made similar calls when he observed the nose of the TOPMS airplane symbol pass corresponding 1,000-foot tick marks along the edge of the runway graphic. The correlation was good; consequently, the test series proceeded as planned. A second opportunity for this type of calibration check occurred at Patrick Air Force Base on the third test day. Those results were similarly good.

## Test Runs

Eighty-five test runs (55 takeoff and 30 abort situations) were made with the TSRV. The test conditions and runs are summarized in Table 5 (page 17).

In addition to the test situations listed in Table 5, incorrect and inconsistent data were intentionally entered for the pretakeoff calculations to demonstrate that the algorithm was configured to detect unscheduled flap settings, out-of-range or inconsistent inputted data, and runway lengths that were less than the minimum required for the takeoff. Erroneous data were purposely entered at the beginning of each test day; the resulting TOPMS displays (Figure 8 and Figure 9, page 10) were observed several times by the TOPMS pilot.

Because of tire and brake wear and the potential dangers associated with high-speed aborts, the flight test situations

**TOPMS Display with Serious Disagreement Between Indicated and Measured EPRs**

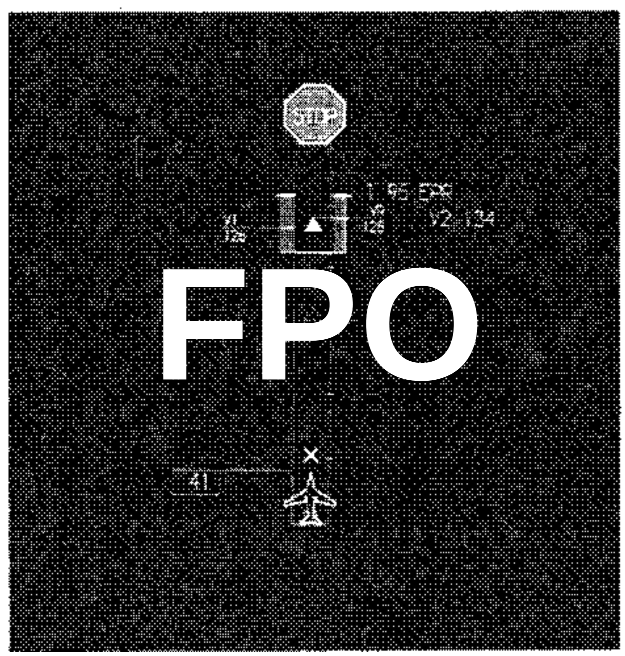


Source: U.S. National Aeronautics and Space Administration, Langley Research Center

**Figure 18**

were designed so that most of them were terminated as takeoffs. For example, after an abort SAF (STOP sign) appeared for several seconds during deficient acceleration runs created by full deployment of spoilers during the takeoff roll, the test director declared an end to the run; the pilot flying lowered the spoilers and completed a pre-planned takeoff. In situations that simulated engine failures, the STOP sign appeared and was observed briefly by the TOPMS pilot who then instructed the pilot flying to complete another pre-planned takeoff. As a consequence of such test procedures, the symbology for takeoff-roll and abort situations was sufficiently exercised and observed by the TOPMS pilot. All TOPMS displays were recorded on videotape, but very few complete sets of numerical test data were obtained.

The primary results from the TOPMS flight tests were observations of the display responses to various operational and environmental conditions. The displays were monitored in real time by all three authors and by the TOPMS pilot.

## Evaluation by TOPMS Project Pilot

In the opinion of the TOPMS pilot who had served as the TOPMS project pilot since the beginning of the simulation evaluation studies,[9,10,12] a highly successful transfer of TOPMS technology was made from the TSRV B-737 simulator to the TSRV airplane. The pilot further indicated that the displays observed in this study performed like those evaluated in the simulation studies. Other comments and observations are paraphrased as follows:

- The TOPMS on-line pretakeoff calculations that yielded the values of velocities $V_1$, $V_R$ and $V_2$ and scheduled EPR were done quickly and precisely. They yielded the same values as those that the pilot flying obtained from the TSRV flight manual for each of the various conditions. In addition, the algorithm appeared to correctly position the performance triangle on the runway graphic at the location where $V_1$ and $V_R$ would be reached.

- During normal takeoffs, setting the throttles according to the scheduled EPR bars produced the proper accelerations needed for the analog airplane graphic to reach the shaded performance triangle at its pretakeoff-predicted location (i.e., the two triangles remained superimposed). This performance inspired confidence in the ability of the algorithm to provide good position information in off-nominal situations.

- Deviations from nominal values of weight, thrust and drag yielded the expected responses in the performance of the TOPMS analog display elements (viz., the airplane symbol, CAS line, shaded triangle, EPR bars and continually updated stop points). In most situations, response changes could be attributed to improper throttle setting or to some other cause.

**TOPMS Displays for Three Braking Levels**

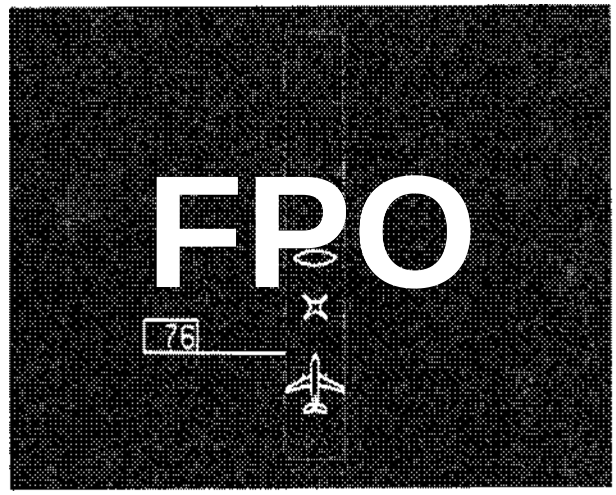


**(a) Partial braking**

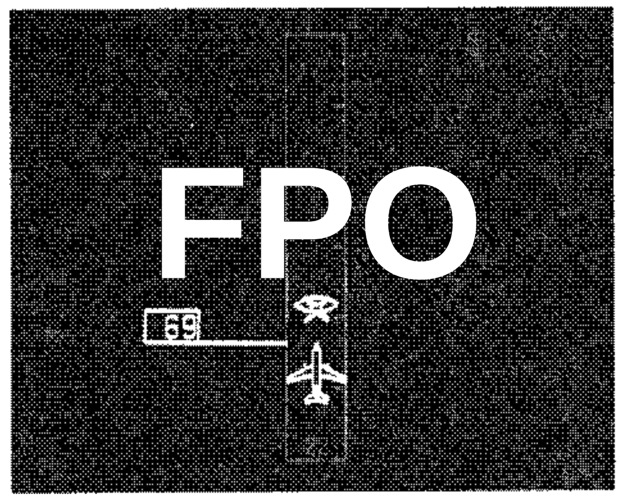


**(b) Full braking, without reverse thrust**

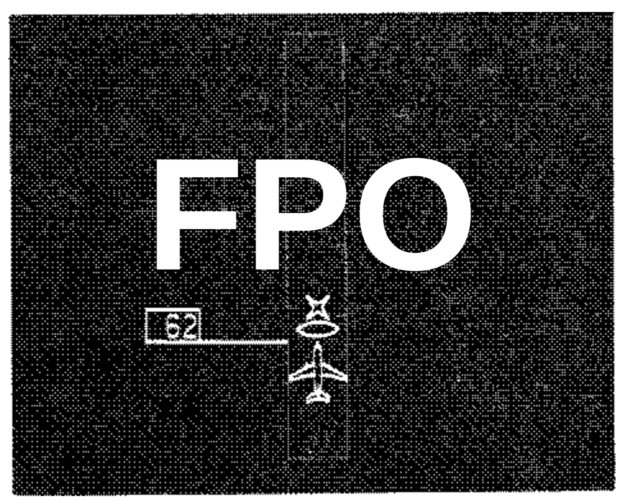


**(c) Full braking, including reverse thrust**

Source: U.S. National Aeronautics and Space Administration, Langley Research Center

**Figure 19**

- The SAFs report the algorithm overall analysis of the situation. It is hoped that the pilots would make the same GO/NO-GO decision without the aid of the SAF, although in some situations the decision might not be made as quickly. If the decision were NO-GO, the earlier in the takeoff roll that it is made, the easier and safer the abort will be.

- In a sense, the SAFs act as a prompter to alert the TOPMS pilot to quickly scan the distributed information for substantiation of the GO or NO-GO advisory before announcing a recommendation to the pilot flying. In turn, the pilot flying should be able to make an earlier and more confident decision.

- Whereas the issue of providing pilots with SAFs and associated activation logic may be somewhat controversial, the TOPMS algorithm has demonstrated flexibility in regard to if, when and how such advisories are presented. Some or all of the SAFs can be omitted without significantly or adversely affecting the more fundamental distributed information (e.g., information on the acceleration performance trend provided by the triangles) .

- The amber SAF should be removed from consideration; it appears on the screen at a critical time when new advice is inappropriate.

- During abort situations, transition from the takeoff display to the abort display with throttle retardation was very quick, smooth and comprehensible. No visual continuity was lost and no mental reorientation was required.

- The correlation was good between the football symbol (instantaneously predicted stop point) and perceived deceleration during both maximum- and partial-braking maneuvers.

The displays for all runs were recorded on videotape for later viewing and correlation with the recorded numerical data and oral comments.

**Functional Block Diagram of Test System**

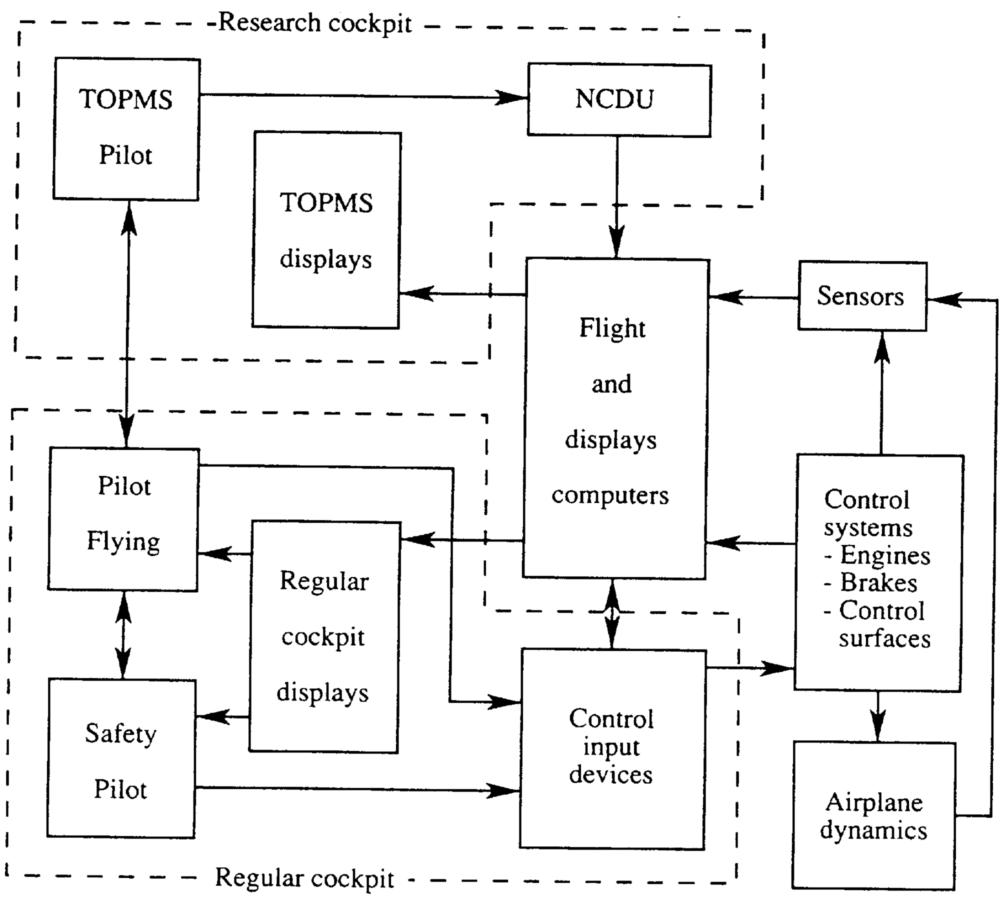


Source: U.S. National Aeronautics and Space Administration, Langley Research Center

**Figure 20**

**Table 5**
**Number of Runs at Various Test Situations**

| | Runs with IMU used on test day | | | Runs with ADIRS used on test day | Runs with body-mounted accelerometer used on test day | | | |
|---|---|---|---|---|---|---|---|---|
| **Test Situation**[1] | 1 | 2 | 3 | 4A | 4B | 5 | 6 | **Total Runs** |
| **Takeoffs** | | | | | | | | |
| 1. Normal | 4 | 3 | 3 | 5 | 5 | 4 | 2 | 26 |
| 2. Low-thrust setting | 1 | 2 | 4 | 1 | 2 | 3 | | 13 |
| 3. Low, then normal thrust | | 1 | 1 | | 3 | 1 | | 6 |
| 4. Large μ-error correction | 1 | 2 | | | | | 2 | 5 |
| 5. Large wind-error correction | 2 | 2 | | | | | 1 | 5 |
| **Aborts** | | | | | | | | |
| 6. Intentional | 1 | 1 | | | | | 1 | 3 |
| 7. Unacceptable acceleration deficiency | | 1 | 4 | | 2 | 2 | 1 | 10 |
| 8. Simulated engine failure | 1 | 3 | 7 | | 1 | 3 | 2 | 17 |
| **Totals** | 10 | 15 | 19 | 6 | 13 | 13 | 9 | 85 |

[1]**Test Situations:**

1. In addition to normal takeoffs at the test sites, data were obtained for all takeoffs going to and returning from these sites; consequently, approximately 30 percent of the runs listed in Table 5 were normal takeoffs.
2. Low-thrust takeoffs were made with EPR settings of 1.6 and 1.7 rather than the nominal EPR settings of 1.88 to 1.95.
3. These runs were begun with significantly lower-than-nominal throttle settings; during the takeoff roll, the pilot flying deliberately moved the throttles up and down several times so the TOPMS pilot could observe the response of the shaded triangle as it continually updated the position for reaching $V_R$.

4,5. One-time adjustments to $\mu_r$ and head wind were automatically made (if necessary) on all runs. Nevertheless, to make this feature noticeable to the TOPMS pilot, intentionally large $\mu_r$ and wind errors were manually entered for several pretakeoff computations. Subsequent throttle adjustments translated to the display as small movements of the shaded triangle each time the throttles were reset and remained stationary for more than three seconds.

6. Three runs were intentionally aborted and the airplane was stopped with maximum-braking application; the laser tracker at the Wallops Flight Facility tracked the airplane during two of the stops.
7. Ten takeoff rolls were made with the spoilers fully deployed to create excess drag as airplane speed increased. In response, the shaded triangle was observed to creep forward until the resulting acceleration error tripped the abort SAF (Figure 17, page 14).
8. Engine failures were simulated when the safety pilot appropriately moved one throttle to artificially induce an EPR discrepancy. For this test only, the algorithm compared the EPR value associated with the current deflected throttle position and its initial target value. Such failures were detected by the TOPMS pilot as a shrinking red EPR bar and an accompanying abort SAF (front cover).

Source: U.S. National Aeronautics and Space Administration, Langley Research Center

## Acceleration Comparisons

In addition to the pilot conversations and comments, several performance variables were recorded for use in real-time and postflight analyses. These analyses involved acceleration time-history comparisons and continual determination of the airplane position on the runway based on several measurement and computational techniques.

Figure 21 (page 18) shows an example of the along-track acceleration measured by the ADIRS sensor unit. Also shown is the reference acceleration that was computed by the

## Comparison of TOPMS Reference and ADIRS Along-track-acceleration Signals During Normal Takeoff Roll

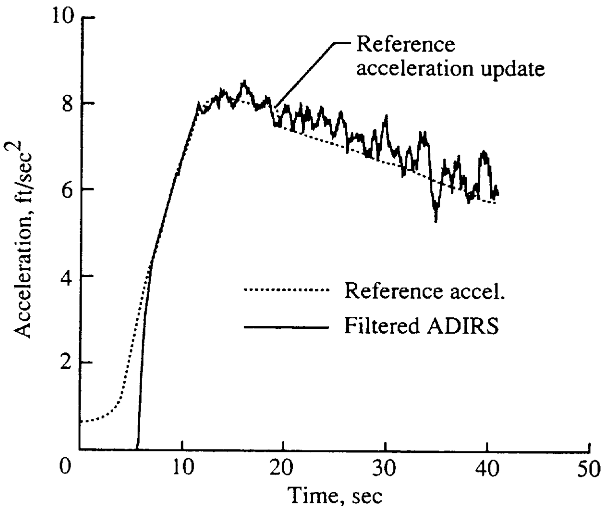


Source: U.S. National Aeronautics and Space Administration, Langley Research Center

**Figure 21**

## Enlargement of Figure 21 Reference Acceleration Adjustment

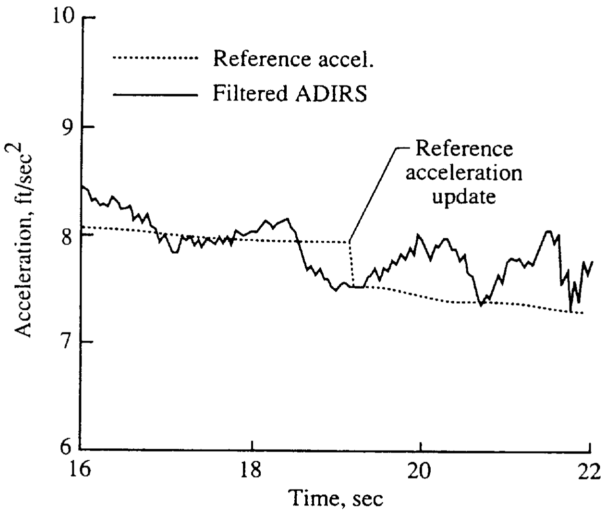


Source: U.S. National Aeronautics and Space Administration, Langley Research Center

**Figure 22**

algorithm for a normal takeoff roll under the same conditions. The ADIRS-measured acceleration signal oscillated within a moderately large envelope. (Subsequently it was judged to be a poor representation of the actual airplane acceleration.) This oscillation, which caused some unexpected SAF display problems, is illustrated in Figures 21–23 (pages 18, 19). The algorithm one-time adjustment of the magnitude of the reference acceleration to that of the measured acceleration came at a time (approximately 19 seconds into the takeoff roll) when the ADIRS curve was in one of its valleys; consequently, the algorithm demanded a large step change in the reference acceleration curve to match that of the ADIRS-measured acceleration. Figure 22 shows an enlargement of the Figure 21 curves in the adjustment region. After the step change, the reference acceleration curve continues along a path parallel to its original path (unless the throttles are again moved or an engine fails). Notice that the corrected reference curve skirts along the bottom boundary rather than through the middle of the ADIRS acceleration envelope.

To determine the acceptability of a particular takeoff-roll performance, a selected acceleration-error band that extends 10 percent above and below the reference acceleration curve was programmed for the flight tests. This band is shown in Figure 23 for the ADIRS reference curve shown in Figure 21. Observe that the measured along-track acceleration exceeded the ±10-percent error band of the reference acceleration several times during the course of the run. To illustrate the problem, a segment of the discrete logic signal that controlled the SAFs during the flight test in Figure 21 has been merged in time across the top of Figure 23. As shown, three abort SAFs flashed on for approximately one second, which resulted in distraction and concern even though no actual acceleration problem existed.

In Figures 21 and 22, observe that had the acceleration adjustment for match up occurred about one second later, a small upward movement in the reference signal would have occurred and most likely would have shifted the upper error band high enough to preclude the three on-off abort SAF flashes. Nevertheless, a large downward excursion of the ADIRS signal at approximately 34 seconds (Figure 23) would probably have caused a single flash of the abort SAF.

Figure 24 (page 20) shows the concurrently measured (but unused) acceleration signal from the TSRV bodymounted x-axis accelerometer during the same run (Figures 21–23). Note that this signal did not have large oscillations; if it had been used as the input to the TOPMS algorithm for this run, the effect of the wind and $\mu_r$ adjustments at 19 seconds would have been hardly noticeable. Further note that if a ±10-percent error band had been drawn for this reference curve, the acceleration measured by the body-mounted accelerometer would have been easily contained within it.

The following two software patches, which were coded and approved by safety personnel before the flight, were temporarily installed in the TOPMS software to alleviate the nuisance SAF problem that occurred when the ADIRS acceleration measurement was used to drive the TOPMS displays:

1. A digital counter prevented the appearance of an abort SAF because of out-of-range, along-track acceleration

**Abort Flag Occurrences due to ADIRS Along-track-acceleration Signal Excursions Outside ±10 Error Band (n = 5)**

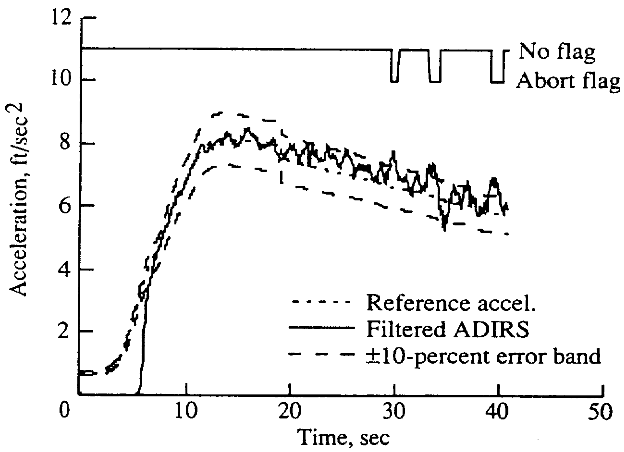


Source: U.S. National Aeronautics and Space Administration, Langley Research Center

**Figure 23**

unless the signal remained out of range during several consecutive (or nearly consecutive) data samples (sample rate of 20 per second).

2. The acceleration-error tolerance band was increased from ±10 to ±15 percent.

The out-of-range digital counter functioned as follows. A positive integer (n) was initially set to zero. When the sampled acceleration-error value exceeded the ±10-percent error band in a computation cycle, n advanced one count. If the acceleration signal was still out of bounds on the next computation cycle, n advanced another count; however, if the acceleration signal was back inside the error band, n was reduced one count. Experimental limits were imposed on n; for example, if n = 5 were this limit (corresponding to the acceleration signal being out of bounds for 0.25 seconds), the TOPMS logic would activate an abort SAF only when n = 5. It would remain at n = 5 until the acceleration signal was again within bounds, whereupon n would drop back one count toward zero. When n = 0, it remained there unless another excursion occurred. The n values investigated were 5, 8 and 10. This technique yielded improved results but did not eliminate all the SAF nuisance flashing, even when n was set at 10.

The second software patch expanded the acceleration-error band from ±10 to ±15 percent, which would easily have contained the ADIRS acceleration signal shown in Figures 21–23. Together the two fixes eliminated the nuisance SAFs triggered by the ADIRS signal; the second fix alone probably would have been sufficient and was certainly the most straightforward. In retrospect, the revised ±15-percent limit may be just as appropriate as the arbitrarily selected ±l0-percent limit. Nevertheless, if an airplane is equipped with a sensor package that delivers a reasonably well-filtered along-track acceleration signal, the smaller band should be sufficient. Defining an optimal acceleration-error band was beyond the scope of this investigation.

Figure 25 (page 20) shows measured and reference acceleration for a situation in which the spoilers were intentionally deployed from the beginning of the takeoff roll. Note that as speed increased, the measured acceleration fell below the reference curve (dashed line) as expected. When the algorithm made its check of the acceleration performance just after the throttles were set for three seconds, the measured acceleration was about 0.5 feet (0.2 meters)/second$^2$ below what it nominally should have been for the measured throttle setting. Accordingly, the algorithm changed $\mu_r$ and adjusted the reference acceleration to the measured value at this time. Subsequently, the abnormally increasing aerodynamic drag because of the deployed spoilers continued to cause the measured acceleration to decrease. At about 21 seconds, the algorithm determined that the measured acceleration error had exceeded the ±10-percent limit and it switched on the abort SAF. After the TOPMS pilot briefly observed the SAF, the run was declared complete and the pilot flying lowered the spoilers and made a preplanned takeoff.

## Distance Determination Using Alternative Methods

The TOPMS algorithm computed the TSRV runway positions throughout the flight-test series by double integration of the pretakeoff-predicted (nominal) and the real-time-measured (and filtered) accelerations (Figure 6, page 8). The TSRV positions were referenced to a specified start point whose coordinates were pre-established by land survey. During postflight analysis, filtration and single integration of the independently measured ground speed (method 2 in Figure 6) appeared to provide more accurate runway positioning. This was determined by comparing distances-traveled data obtained by single integration of ground speed, by double integration of acceleration, and by real-time range measurements made with the Wallops Flight Facility ground-based laser tracker. This tracker has a dynamic range accuracy of ±1.65 feet (0.5 meters) (standard deviation) and a pointing accuracy of 0.3 milliradian in azimuth.[14] Unfortunately, the laser tracker was available for only part of one test day.

Because of the variability of flight-test conditions and procedures (including early termination of some runs and/or early cutoffs of data recorders), only six normal takeoff runs had sufficiently complete data sets for strict comparisons of the TSRV positions at $V_R$; the TSRV was tracked by laser radar in only two of these runs, which further restricted comparative data. These data are shown in Table 6 (page 20).

## Comparison of TOPMS Reference and TSRV Body-mounted X-axis Acceleration During Normal Takeoff Roll

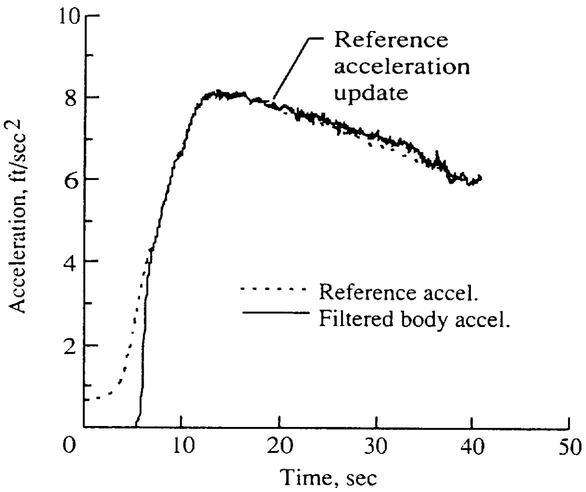


Source: U.S. National Aeronautics and Space Administration, Langley Research Center

**Figure 24**

Runs 1-3 show results when the along-track acceleration input to the TOPMS algorithm came from the TSRV IMU. Runs 4–6 show similar data when the input was obtained using the body-mounted, x-axis accelerometer. No suitable along-track acceleration input signals were obtained from the ADIRS unit.

A comparison of the computed and measured position data is shown in Figures 26–28. In Figure 26 (page 21), six groups of incremental differences in takeoff-roll distances are shown across the bottom and the run numbers common to each group are indicated along the top. With the exception of run 2, the algorithm method 1 computed values of takeoff-roll distances $d_a$ from the TSRV start points to the locations where its airspeed reached $V_R$ were approximately 200 feet (61 meters) less than pretakeoff-roll-predicted distances $d_p$ for nominal conditions. The magnitude of the differences corresponds roughly to two lengths of the TSRV or less than the distance it travels during the last second before reaching $V_R$. Part of the difference can be attributed to $\mu_r$ being updated from the 0.015 assumed nominal value to values ranging from 0.020 to 0.030. Also, the wind inputs were adjusted 2–3 knots upward in all but run 2, where no change occurred. In runs 3–6, the method 2 computations of distance traveled for the TSRV to reach $V_R$ ($d_{gs}$) closely agreed with pretakeoff predictions of $V_R$ positions; method 1 computations showed only fair agreement. Runs 1 and 2 provided mixed support of this trend. In runs 5 and 6, $d_p$ and $d_{gs}$ compared well with the respective laser-tracker measurements ($d_{lt}$).

To provide additional insight, Figure 27 and Figure 28 (page 22) present curve data of the TSRV runway positions during runs 5 and 6, respectively, by using the computational

## Table 6
## Measured and/or Computed Positions of TSRV at $V_R$

| Run | Distance, feet | | | |
|---|---|---|---|---|
| | *$d_p$ | †$d_a$ | ‡$d_{gs}$ | ≈$d_{lt}$ |
| 1 | 3,307 | ¤3,033 | 3,068 | |
| 2 | 3,441 | ¤3,467 | 3,740 | |
| 3 | 3,244 | ¤3,067 | 3,248 | |
| 4 | 3,133 | #2,909 | 3,140 | |
| 5 | 2,637 | #2,452 | 2,631 | 2,690 |
| 6 | 2,645 | #2,427 | 2,634 | 2,696 |

*$d_p$ algorithm-predicted distance from nominal acceleration

†$d_a$ algorithm-computed distance from measured acceleration

‡$d_{gs}$ algorithm-computed distance from measured ground speed

≈$d_{lt}$ measured distance from radar laser tracker

¤ acceleration signal from IMU

# acceleration signal from body-mounted accelerometer

Source: U.S. National Aeronautics and Space Administration, Langley Research Center

## Comparison of Reference and Body-mounted X-axis Acceleration During Takeoff with Excess Drag (Deployed Spoilers)

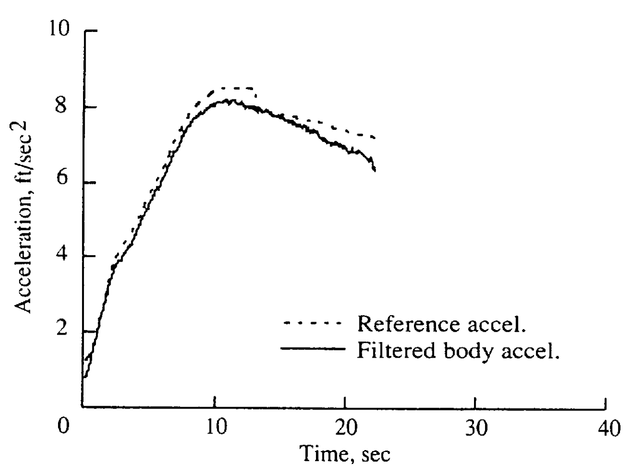


Source: U.S. National Aeronautics and Space Administration, Langley Research Center

**Figure 25**

## Comparison of Laser-tracker-measured and TOPMS-computed Positions of TSRV at $V_R$

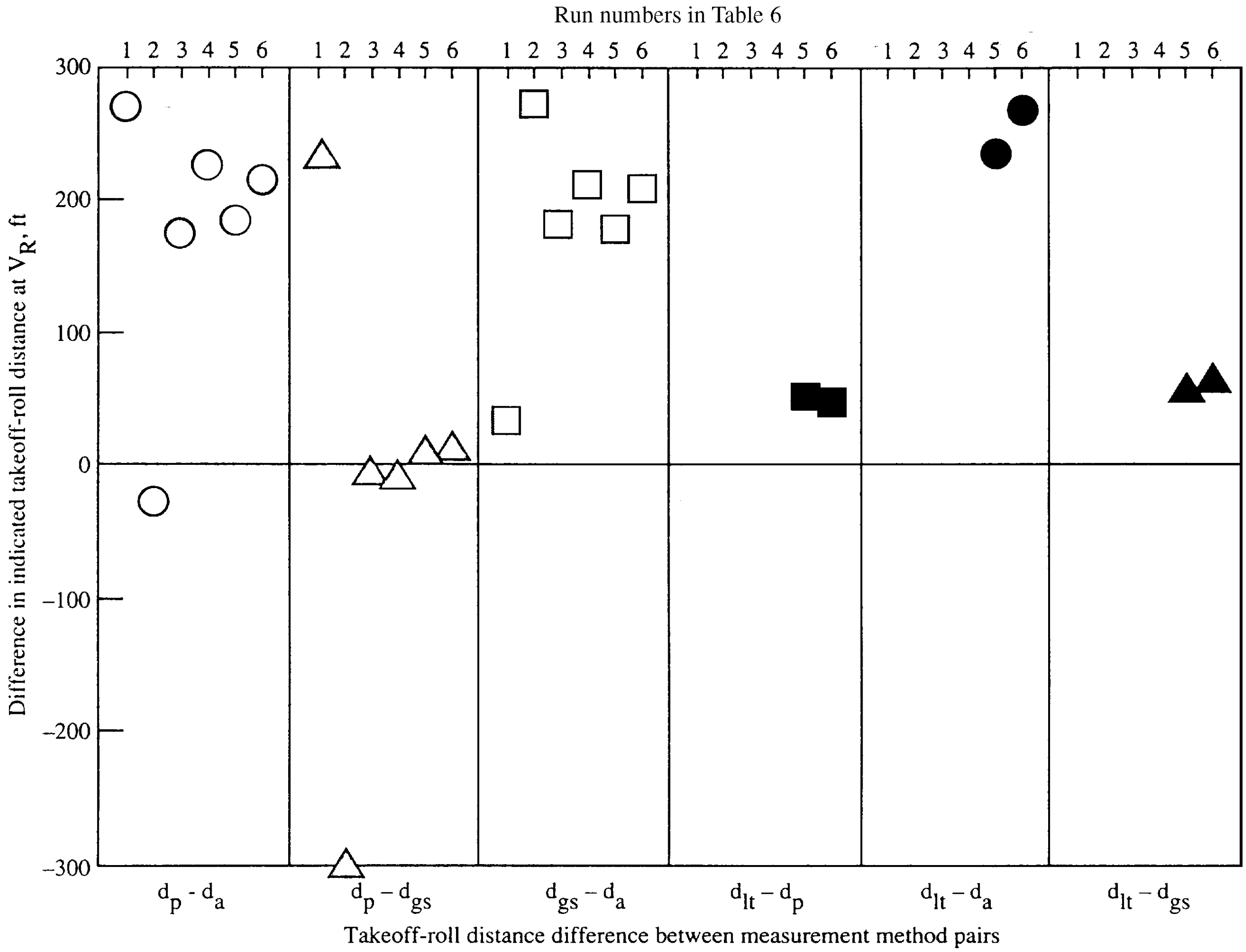


Source: U.S. National Aeronautics and Space Administration, Langley Research Center

**Figure 26**

methods 1 and 2. In Figure 27, the run 5 pretakeoff prediction (2,637 feet [804 meters]) of where the TSRV should reach a speed of $V_R$ under nominal conditions is indicated by the dark circle. The laser tracker-measured distance at $V_R$ (2,690 feet [820 meters]) is indicated by the triangle. The solid and dashed lines show corresponding positions using integration methods 1 and 2, respectively. Both curves end at the location where CAS reaches $V_R$. Similar data for run 6 are shown in Figure 28. Both sets of curves appear to increase smoothly with airspeed, indicating that the distance differences might be attributable to the integration methods rather than any parameter correction anomalies. Nevertheless, not enough data are available to confirm the trend.

The method 1 vs. method 2 pattern was also apparent during a reduced-thrust takeoff from the 2,000-foot (610-meter) altitude commercial runway at Asheville, North Carolina, where no laser tracker was available (Figure 29, page 22). The circle at approximately 3,000 feet (914 meters) down the runway shows the pretakeoff prediction based on the throttle setting that would produce a scheduled EPR of 1.95. However, during this run, the pilot purposely used a throttle setting that produced an EPR of 1.7. The resulting lower acceleration level caused the CAS to increase at a slower pace and, according to method 1, the TSRV reached $V_R$ about 1,000 feet (305 meters) farther down the runway than predicted at pretakeoff; when using method 2, the TSRV position was about 1,200 feet (366 meters) farther down the runway. (Both curves terminate where CAS reaches $V_R$.)

## Aborted Takeoffs

Two maximum-braking aborts were made during tests at the Wallops Flight Facility. The primary purpose was to compare the laser-tracker-measured stopping distances vs. the stopping distances computed by the TOPMS algorithm using methods 1 and 2. Figure 30 and Figure 31 (page 23)

**Comparison of Laser-tracker-measured And Three Computed Positions of TSRV During Run 5 Takeoff Roll**

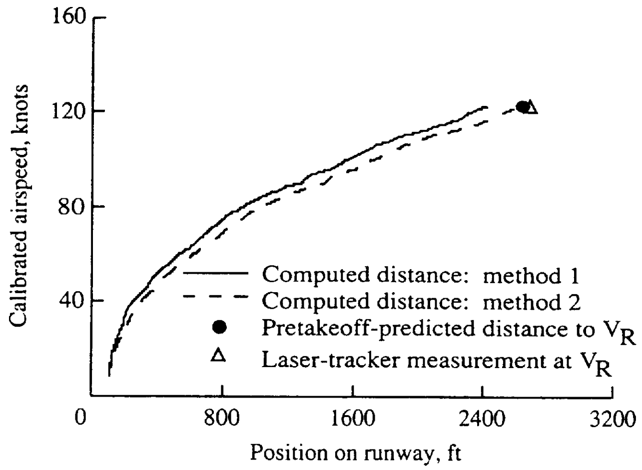


Source: U.S. National Aeronautics and Space Administration, Langley Research Center

**Figure 27**

**Comparison of Laser-tracker-measured And Three Computed Positions of TSRV During Run 6 Takeoff Roll**

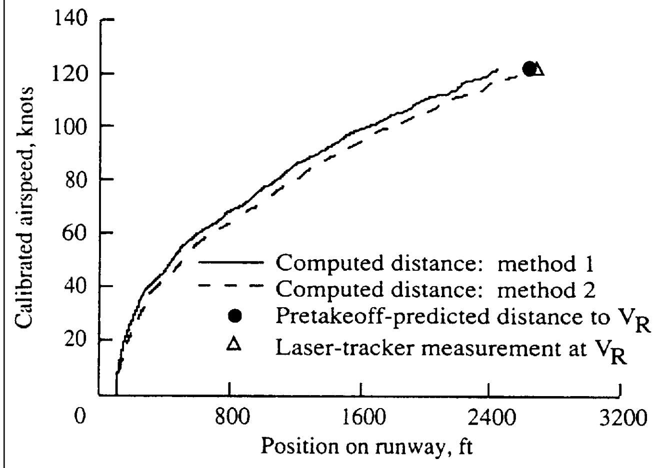


Source: U.S. National Aeronautics and Space Administration, Langley Research Center

**Figure 28**

show this comparison for maximum-braking stops from approximately 80 knots and 100 knots, respectively. The winds were light for both runs so the CAS and ground-speed values were approximately equal.

At the beginning of the 80-knot situation (Figure 30), $\mu_r$ = 0.04 was entered as an intentional error, which the algorithm corrected to $\mu_r$ = 0.016 at approximately 30 knots. At 80 knots, it took about three seconds for the TOPMS pilot to call for the abort and for the pilot flying to respond (i.e., hear the call, reduce the throttles, pull the speed-brake lever and apply the foot brakes); consequently, ground speed reached approximately 86 or 87 knots before braking became the dominant longitudinal force. A comparison of airplane position during the takeoff roll showed the same trend as seen during previous takeoffs (Figure 27 and Figure 28); that is, the laser tracker determined that the position of the airplane was ahead of the TOPMS-computed position. Note that the TOPMS computations and the laser measurements of the braking distance correlated closely; the distance differential at the end of the run was about the same as it had been at abort initiation. (The runs were declared complete when speed was reduced to about 15 knots because the TSRV antiskid brake system ceased operation below this level.)

In the 100-knot situation (Figure 31), the pilot flying reacted more quickly (in slightly less than two seconds) and ground speed reached only about 103 knots when full braking was applied. Laser tracker measurements and method 2 computations of braking distance agreed closely; again, the laser tracker indicated that the TSRV was slightly farther down the runway.

To add interest during another braking run at the Wallops Flight Facility, the TOPMS pilot covertly selected the 2,000-feet- (610 meter-) to-go mark on his runway graphic as a target stop point. Then without informing the pilot flying of the purpose, the TOPMS pilot verbally instructed the pilot flying when to apply more or less braking. The pilot flying obliged and the TSRV was brought to a stop as the nose of the graphic airplane reached the target mark. The TOPMS pilot then asked the safety pilot

**Comparison of Runway Position Computation Methods 1 and 2 During Reduced-thrust Takeoff Run**

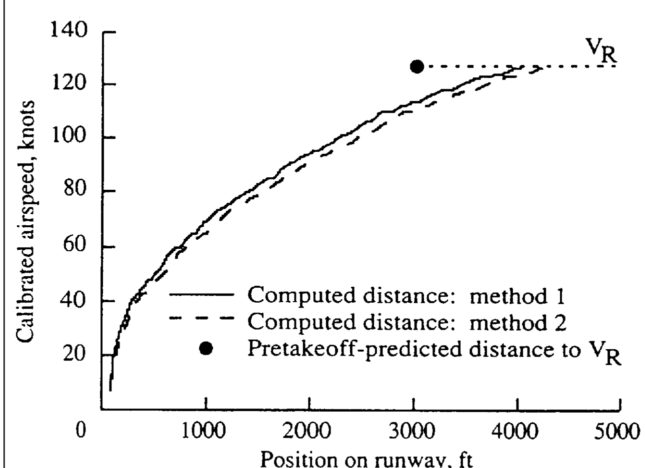


Source: U.S. National Aeronautics and Space Administration, Langley Research Center

**Figure 29**

to look out the side window and report where the airplane had stopped. The TSRV had indeed come to a stop approximately opposite the 2,000-feet-to-go marker sign alongside the runway. Although this was not a planned or rigorous test, it further demonstrated that the TOPMS algorithm was providing reasonably accurate distance information on dry runway surfaces.

The SAFs and predicted stop-point x augment the elemental, distributed TOPMS display with important information concerning both system and acceleration performance. For example, after an engine failure, the pilot must quickly assess the seriousness of the situation and decide whether the airplane can be stopped in the remaining runway distance. A red SAF would instantly advise the pilot that the airplane could probably be stopped; a green SAF would indicate that it most likely could not. The predicted stop-point symbol x would support the SAF in both cases.

An EPR bar that rises to its target (scheduled) mark, turns red, and does not diminish in length indicates a serious mismatch between the measured EPR and the EPR value associated with the measured throttle position. A situation in which both engines are operating with a serious EPR mismatch is illustrated in Figure 18 (page 14). In this figure, the shaded triangle has advanced so far downfield that it has crossed the GRLL. Two violations of TOPMS criteria that have occurred (Table 5, page 17) for continued takeoff are a large EPR vs. throttle-position EPR disagreement and insufficient runway distance remaining for a sanctioned takeoff. Either of these violations would trigger an abort SAF. The following real-world case illustrates this situation.[15]

**Roll Distance Before and Braking Distances After Abort at 80 Knots**

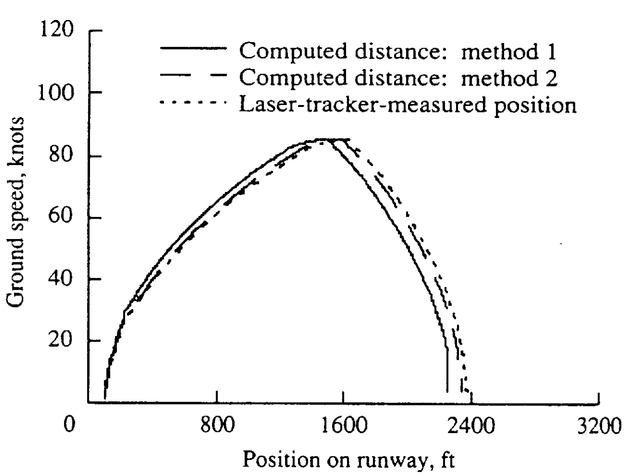


Source: U.S. National Aeronautics and Space Administration, Langley Research Center

**Figure 30**

**Roll Distance Before and Braking Distances After Abort at 100 Knots**

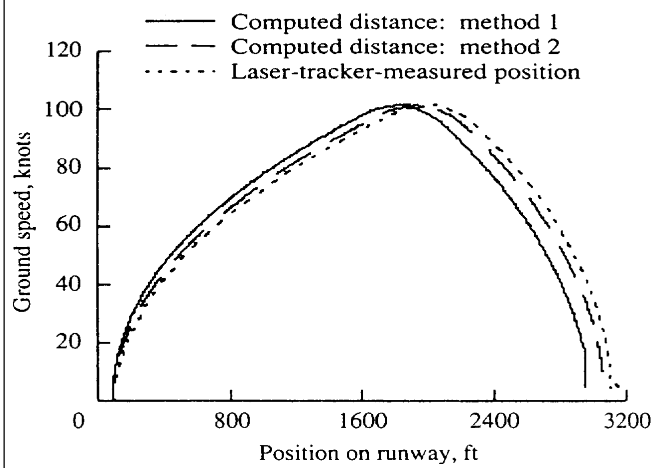


Source: U.S. National Aeronautics and Space Administration, Langley Research Center

**Figure 31**

In January 1982, a heavily loaded Boeing 737-222 attempted to depart from the Washington National Airport (Washington, D.C.) in a heavy snowstorm. For several contributing reasons, the flight ended in a fatal crash soon after liftoff. The runway length was near minimum for the airplane under the existing weather and loading conditions.

If a TOPMS like the one described in this report had been operating aboard that aircraft, it would have provided the pilots with the following information:

1. Before beginning the takeoff roll, the pilot would have set the throttles on zero deflection angle for idle thrust, but the EPR bars on the display would have extended noticeably above their usual zero length, which indicates that greater than idle thrust was being sensed. Engine sound and other cockpit information, however, would not have supported an above-idle-thrust situation and would have alerted the crew of a potentially serious problem.

2. If this visual cue were ignored and the takeoff roll begun, both EPR bars would have risen to their respective target marks in response to the throttle advances, which would have been lower than normal. About three seconds after the throttles were set to match the target EPR marks on the display, both EPR bars would have turned red but retained their target length. Additionally, the algorithm would have reacted to the large mismatch between the target EPR and the EPR value associated with the sensed throttle position by immediately causing an abort SAF and a predicted stop-point x to appear on the runway graphic. The shaded

triangle would also have jumped far down the runway indicating that measured acceleration was significantly lower than the nominal expected for the ongoing maneuver.

3. If the takeoff roll continued, the shaded triangle would have soon crossed the GRLL (shown in Figure 18, page 14), violating yet another abort criterion. (See condition 7 in Table 4, page 8.)

A TOPMS display with fewer features (e.g., no SAF or x ) would also have provided valuable information in the case described above but would not have been as dramatic. The nominal-length red EPR bars would have brought attention to the display; the greatly separated triangles would have indicated graphically that the magnitude of the low-acceleration condition and that the airplane might not attain $V_R$ before it reached the GRLL.

Inclusion of the SAFs in the TOPMS package is not intended to reduce pilot responsibility in deciding on a course of action (i.e., GO or NO-GO). The SAFs provide an instant second opinion that a problem that requires action may exist based on the algorithm's logical analysis of existing parametric values and other data related to programmed criteria. Whereas the SAFs may not be perceived as stop-priority (or necessary) information by highly experienced pilots (such as the TOPMS pilot in this study), the SAFs would provide valuable and timely cues for less experienced pilots; the SAFs would prompt them to immediately scan the supporting information to verify a real or potential problem and quickly decide on the appropriate control response (i.e., make the GO/NO-GO decision as early as possible).

An alternative to the abort SAF in this situation could be an acceleration-error indicator (e.g., the one used in the TOPMS HUD in the reference 16 simulation study). Inclusion of either the abort SAF or an acceleration-error indicator should facilitate early investigation of the cause of the shaded triangle displacement away from the predicted $V_R$ point (i.e., lower-than-nominal throttle setting, EPR-bias errors or excessive drag). The presence of either symbol (or both) also relieves the pilot from having to closely or continuously watch the shaded triangle.

For completeness, the amber SAF (Table 4, page 8 and Figure 15, page 13) was flight tested; however, it is being deleted from the TOPMS for lack of sufficient pilot support in this and in previous studies.[11]

The TOPMS runway tests indicated to the test team that the simulator-developed TOPMS technology had been successfully transferred to the TSRV. The algorithm was easily installed on the TSRV regular graphics computer. It reliably calculated the TSRV performance and accurately provided a graphical display of the runway situation expected under a variety of nominal and error conditions (i.e., induced acceleration deficiencies; simulated engine failures; and several runway, gross-weight, temperature, wind, pressure and altitude conditions). The TOPMS also interfaced well with other onboard equipment through the airplane's all-purpose, high-speed data bus.

Although quantitative data gathering was not a primary test objective, some preliminary distance comparisons were extracted from recorded flight data. In particular, the following trends were observed:

- When roll distances required to reach takeoff speed $V_R$ were computed from accelerometer measurements, they were typically two airplane lengths less than (a) pretakeoff-predicted distances computed from nominal acceleration, (b) distances measured by a ground-based laser radar tracker and (c) distances computed from independently measured ground speed.

- The computed and measured braking distances appeared to be in better agreement than the takeoff-roll distances; however, additional data are needed to confirm this.

Based on the results of these runway tests, the following recommendations concerning the TOPMS algorithm and displays are listed:

- A study should be made to determine the optimal magnitude of the error band about the reference acceleration to prevent unwarranted or nuisance abort advisories. This study illustrated that a ±10-percent error band should be sufficient when well-filtered, along-track accelerometer signals are available; however, this error band may not adequately encompass all of the possible nuisance anomalies.

- The $\mu_r$-update feature could be removed because it appears to provide very little practical benefit; in fact, in some instances, it may be counterproductive.

- The GO and NO-GO SAFs should be retained as active elements of the TOPMS displays. The TOPMS displays provide desirable basic performance information without them, but the SAFs appear to be a positive enhancement.

4. An accurately measured ground-speed signal, when available on a particular airplane, should be considered as the TOPMS input for the real-time distance computation of the airplane position. This computational technique, however, also needs more extensive study.

The TOPMS is operational and has been retained on the TSRV for general use and demonstration. It would, however, be desirable to demonstrate and evaluate the TOPMS on another airplane with different characteristics, sensors and support equipment (e.g., a head-up display). The TOPMS software could be adapted and used to advantage on any modern airplane equipped with digital flight-control computers. ♦

[Editorial note: This article has been adapted from the U.S. National Aeronautics and Space Administration Technical Paper 3403, *Flight Test of Takeoff Performance Monitoring System*. May 1994, Langley Research Center, Hampton, Virginia, U.S.]

## References


1. Bacqué, Peter. "NASA Offers Airline Pilots Aid." *Richmond Times-Dispatch*, Nov. 12, 1989: C–8.

2. Minutes of Meeting #1 of the Take-Off Performance Monitoring Ad Hoc Committee. Aircraft Div., Aerospace Council, Soc. of Automotive Engineers, Inc. (Washington, D.C.) May 15–16, 1984.

3. Fusca, James A. "Takeoff Monitor Computes Runway Roll." *Aviation Week & Space Technology*. Volume 69 (Oct. 13, 1985): 99–100 and 103–105.

4. Compania de Transport Aerian Tarom (Ioan Aron and Ion Tomescu): Take-Off Director System. U.S. Patent No. 4,251,868, Feb. 17, 1981.

5. Small, John T. Jr. "Feasibility of Using Longitudinal Acceleration ($N_x$) for Monitoring Takeoff and Stopping Performance From the Cockpit." In *The 1983 Report to the Aerospace Profession — 27th Symposium Proceedings.* Society of Experimental Test Pilots, 1983.

6. Boeing Co. (Patrick J. Cleary, Lloyd S. Kelman, and Richard L. Horn): Aircraft Performance Margin Indicator. European Patent Application No. 85200977.8, Publication No. 0 166 487 A2, June 19, 1985.

7. Srivatsan, R. "Design of a Takeoff Performance Monitoring System." Ph.D. thesis, University of Kansas, 1985.

8. Srivatsan, R.; Downing, D. R.; Bryant, W. H. *Development of a Takeoff Performance Monitoring System.* U.S. National Aeronautics and Space Administration TM-89001, 1986.

9. Middleton, David B.; Srivatsan, Raghavachari; Person, Lee H. Jr. *Simulator Evaluation of a Display for a Takeoff Performance Monitoring System.* U.S. National Aeronautics and Space Administration TP-2908, 1989.

10. Middleton, David B.; Srivatsan, Raghavachari; Person, Lee H. Jr. "Simulator Evaluation of Takeoff Performance Monitoring System Displays." In *A Collection of Technical Papers — AIAA Flight Simulation Technologies Conference.* Sept. 1988: 206–214. (Available as AIAA-88-4611-CP.)

11. *Airworthiness Standards: Transport Category Airplanes.* U.S. Federal Aviation Regulations Part 25, U.S. Federal Aviation Administration. June 1974.

12. Middleton, David B.; Srivatsan, Raghavachari; Person, Lee H. Jr. *Simulator Evaluation of Displays for a Revised Takeoff Performance Monitoring System.* U.S. National Aeronautics and Space Administration TP-3270, 1992.

13. Bruce, Kevin R. *NASA B737 Flight Test Results of the Total Energy Control System.* U.S. National Aeronautics and Space Administration CR-178285, 1987.

14. NASA Langley Research Center and Boeing Commercial Airplane Co. *Terminal Configured Vehicle Program — Test Facilities Guide.* U.S. National Aeronautics and Space Administration SP-435, 1980.

15. *Aircraft Accident Report — Air Florida, Inc., Boeing 737-222, N62AF Collision With 14th Street Bridge, Near Washington National Airport, Washington, D. C., January 13, 1982.* U.S. National Transportation Safety Board AAR-82-8, Aug. 10, 1982. (Available from National Technical Information Service as PB 82 910 408.)

16. Middleton, David B.; Srivatsan, Raghavachari; Person, Lee H. Jr. "Takeoff Performance Monitoring System Display Options." In *A Collection of Technical Papers — AIAA/AHS Flight Simulation Technologies Conference.* August 1992: 57–67. (Available as AIAA-92-4138.)

## Aviation Statistics

# Turbulence Accidents Increased in 1993 Over Previous Five Years

***The 1993 rate for pushback accidents was lower than that for five- and 35-year periods.***

*Editorial Staff*

*Commercial Jet Transport Safety Statistics 1993* examines commercial aviation's safety record not only for 1993 but for the five-year period 1989-1993 and the 35-year span from 1958, at the beginning of the jet transport era, to 1993.

Among the specifics presented in the study, published by McDonnell Douglas, are those for "excluded accidents," that is, those with characteristics that caused them to be eliminated from mainstream accident data; for accident sources subdivided according to personnel; and for accidents involving unsafe acts.

Excluded accidents (Figure 1, page 28) fall outside the parameters for accidents considered elsewhere in the study. "They are those," said the report, "in which neither the aircraft's equipment, crew, nor flight operational procedures were factors in the accident." Examples included towing or pushback mishaps, ground collisions in which the aircraft was struck by another object such as a jetway, servicing accidents and terrorist acts. Under this definition, a full 26 percent of all aircraft accidents were excluded in the rest of the study.

During the 35-year period, turbulence was responsible for the largest number (164) of these accidents. The study defined an accident as when "any person suffers death or serious injury as a result of being in or upon the aircraft, or by direct contact with the aircraft or anything attached thereto." The next highest incidences were associated with pushbacks (56), followed by emergency evacuations (51).

Rates for these three most common types of "excluded" accidents were studied for the 1989-1993 period and for 1958-1993 (Table 1, page 27). Turbulence-related accidents showed exactly the same rate (0.42 per million flight hours) in 1993 as in the 35-year survey, although the rate was lower (0.20) for the five-year span. The 10 turbulence-related accidents in 1993 represented a larger number than in any of the previous four years.

Although pushback accidents have received more attention recently (*Airport Operations*, May-June/July-August 1994), the 1993 rate (0.15 per million departures) was lower than that for either the five-year period (0.44) or the 35-year period (0.22). The rate for emergency-evacuation accidents varied little among the 1993, five-year or 35-year periods studied.

The study examined the numbers of various types of personnel who were accident sources in 1993 and from 1958 through 1993 (Figure 2, page 29). "Source" was defined as "the thing, person or circumstances that precipitates an event."

Captains scored highest as accident sources among all personnel both in 1993 and throughout the 35-year period, according to the data. In the 710 cases total where the captain was cited as the accident source, the majority of lapses were listed as "execution of action less than adequate" (499), followed by "judgment less than adequate" (266) and "failure to follow proper procedure" (131).

The captain was an accident source in 80 percent of the total number of citations (888) from 1958 through 1993. (Because any given event could involve more than one person, this does not mean that the captain was necessarily the sole source of 80 percent of the accidents.) The corresponding figure for 1993 only was 22 out of 28, or virtually the same (79 percent).

In 1993 as in the 1958-1993 span, first officers represented the second largest group of accident sources. Among other personnel, there were some differences between the single-year and 35-year totals. Ground crew were cited as sources 18 times, out of a total of 888 (2 percent) during the longer period, but did not appear in the 1993-only figures. Neither did maintenance or other flight deck personnel, who were cited as accident sources 13 and nine times, respectively, during the 1958-1993 period.

The breakdown of "accidents involving unsafe acts" (Figure 3, page 30) also showed occasional frequency contrasts between the 1993 single-year and 1958-1993 statistics.

In 1993, the most frequent unsafe acts cited were failure to maintain directional control (six instances), followed by failure to go around, facilities inadequate, and failure to monitor weather (four citations each). During the 1958-1993 period, the most frequent unsafe acts cited were failure to monitor instruments (126), failure to maintain directional control (119) and improper instrument approach. Of those categories, both the first and third ranked relatively low in 1993 alone (two instances and one instance, respectively.)

Comparisons of the 1993 vs. long-term data in these three areas cannot be taken as evidence for any trend, because random variations cancel out the statistical significance of any one year's figures.

The study included only Western-built jet airliners, and did not state whether there were any restrictions on country of registration. ♦

**Table 1**
**Rates for Three Most Common Types of "Excluded" Accidents**
**1958–1993**

| | TURBULENCE | | PUSHBACK | | EVACUATION | |
|---|---|---|---|---|---|---|
| | Events | Rate* | Events | Rate* | Events | Rate* |
| **1993** | 10 | .42 | 2 | .15 | 3 | .22 |
| **Last 5 years** | 22 | .20 | 29 | .44 | 15 | .23 |
| **All years** | 164 | .42 | 56 | .22 | 51 | .20 |

*** Per million departures**

Source: McDonnell Douglas

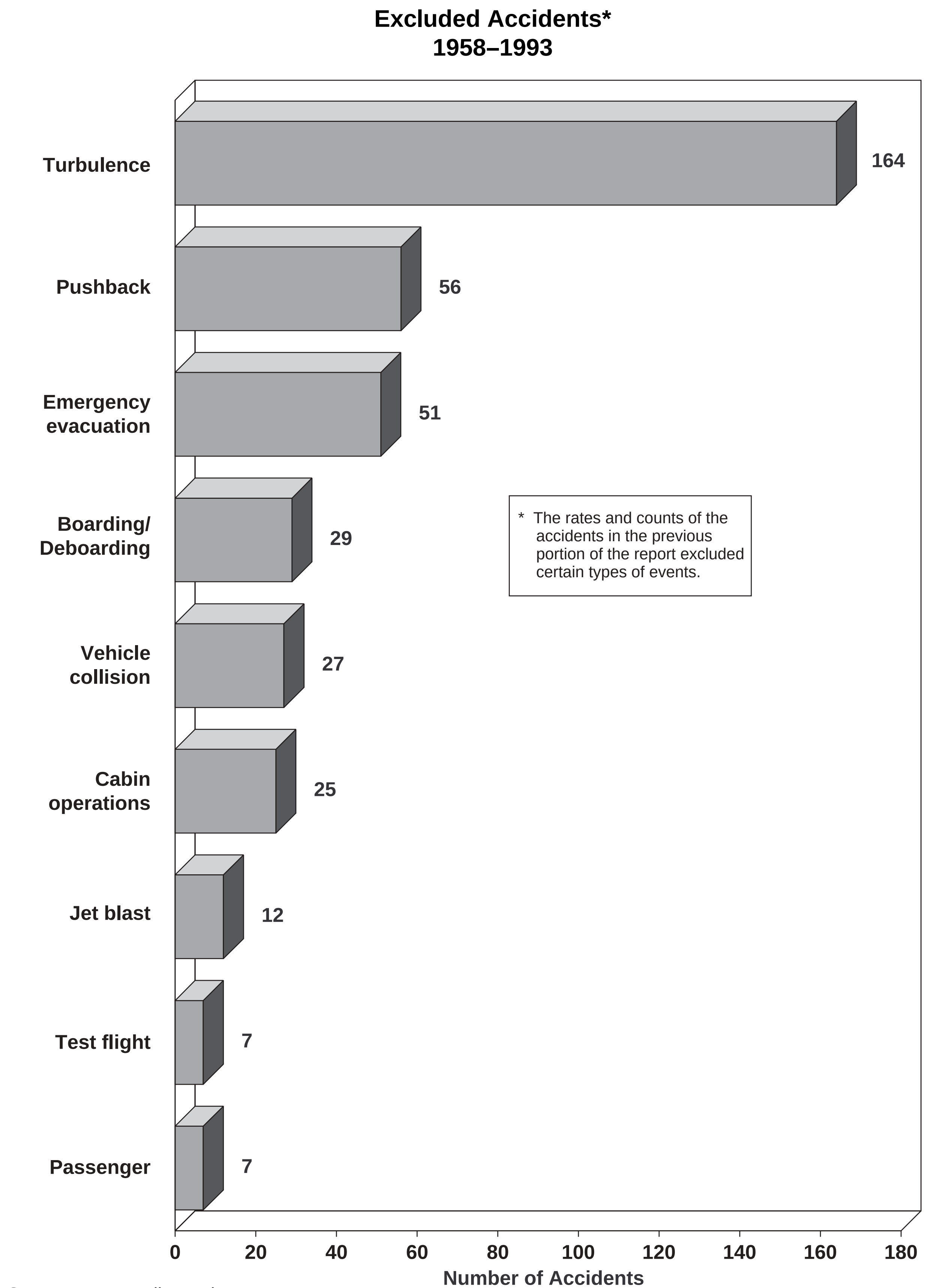


Source: McDonnell Douglas

**Figure 1**

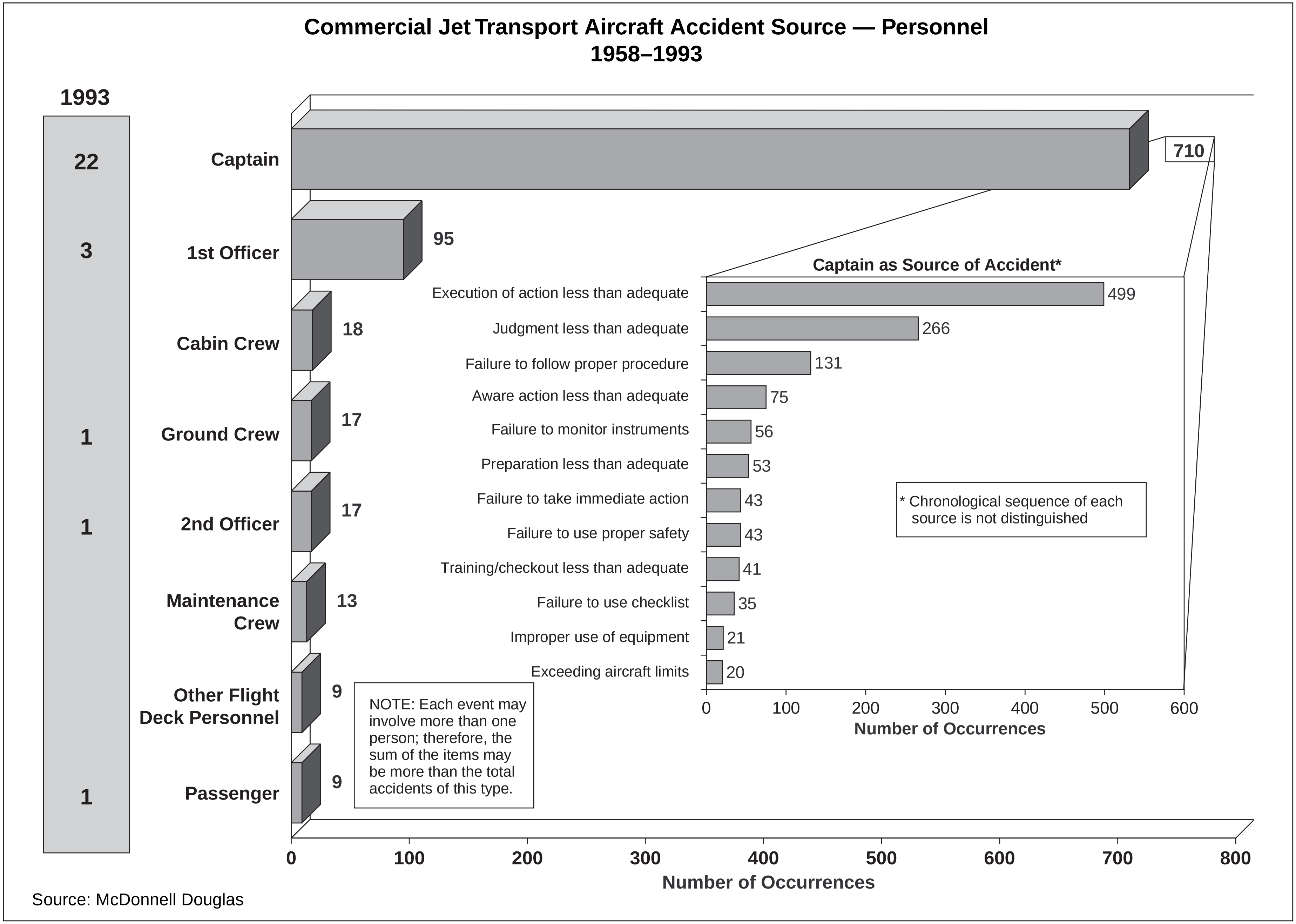

Commercial Jet Transport Aircraft Accident Source — Personnel
1958–1993
1993
22
3
1
1
1
Captain
1st Officer
Cabin Crew
Ground Crew
2nd Officer
Maintenance Crew
Other Flight Deck Personnel
Passenger
710
95
18
17
17
13
9
9
Captain as Source of Accident*
Execution of action less than adequate 499
Judgment less than adequate 266
Failure to follow proper procedure 131
Aware action less than adequate 75
Failure to monitor instruments 56
Preparation less than adequate 53
Failure to take immediate action 43
Failure to use proper safety 43
Training/checkout less than adequate 41
Failure to use checklist 35
Improper use of equipment 21
Exceeding aircraft limits 20
0 100 200 300 400 500 600
Number of Occurrences
* Chronological sequence of each source is not distinguished
NOTE: Each event may involve more than one person; therefore, the sum of the items may be more than the total accidents of this type.
0 100 200 300 400 500 600 700 800
Number of Occurrences
Source: McDonnell Douglas


**Figure 2**

## Commercial Jet Transport Aircraft Accident Involving Unsafe Acts
## 1958–1993

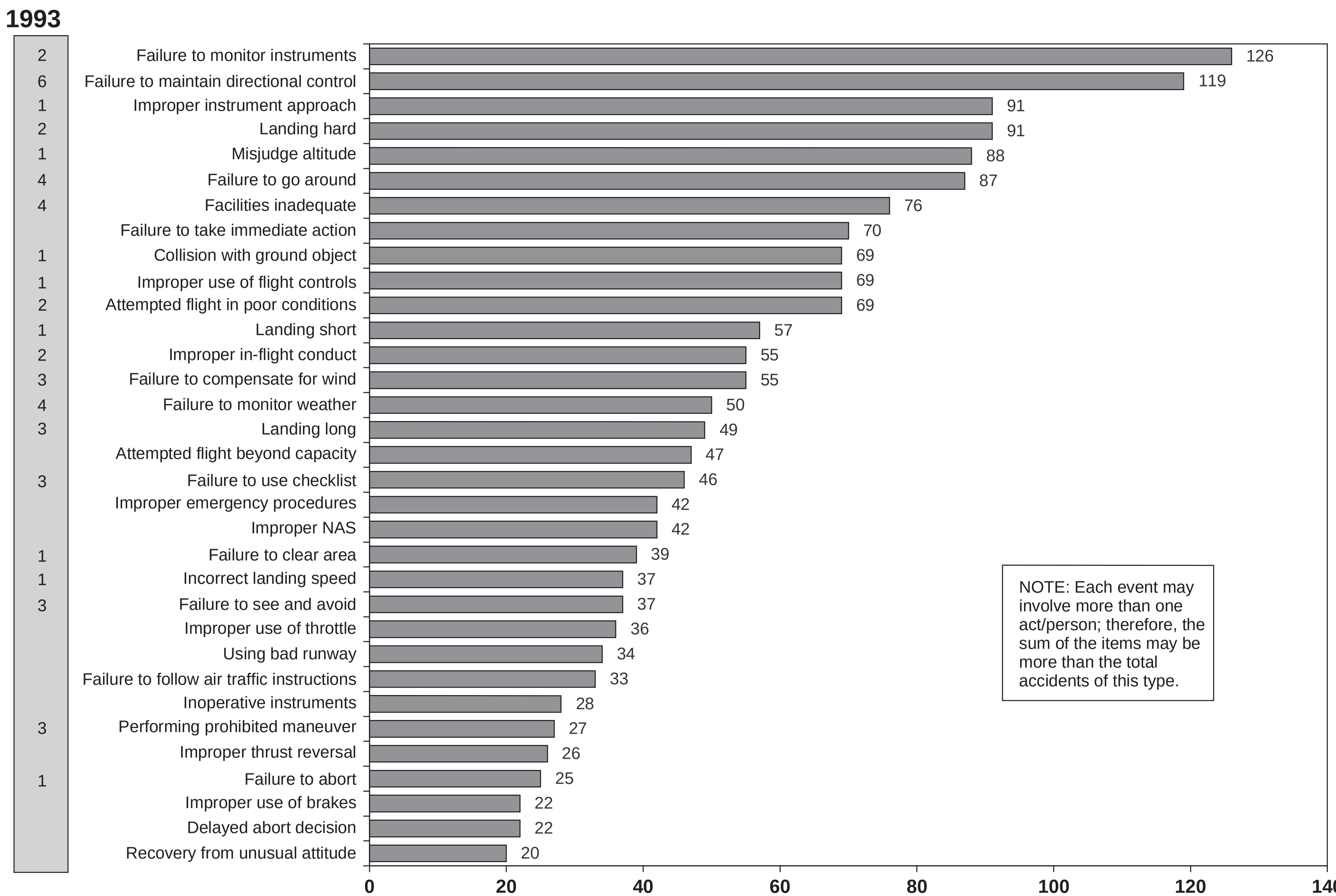


Source: McDonnell Douglas

**Figure 3**

# Advisory Circular Outlines One Method of Obtaining Approval for GPS Navigation Equipment

***Another study analyzes exposure of passengers to cold after being doused with cabin water spray systems.***

*Editorial Staff*

## Reports

*Airworthiness Approval of Global Positioning System (GPS) Navigation Equipment for Use as a VFR and IFR Supplemental Navigation System.* U.S. Federal Aviation Administration (FAA). Advisory Circular (AC) No. 20-138. May 1994. 35 p.; appendices.

Summary: The global positioning system (GPS) is a satellite-based radio navigation system that determines precise position anywhere in the world by using range measurements from GPS satellites. The U.S. Department of Defense (DOD) operates and monitors the satellites. This AC outlined one method of obtaining airworthiness approval for using GPS equipment as a supplemental navigation system for oceanic and remote, domestic en route, terminal and nonprecision instrument approach (except localizer, localizer directional air [LDA] and simplified directional facility [SDF] operations). Only approval of stand-alone GPS equipment was discussed. The AC did not address GPS equipment incorporating differential GPS capability. [from purpose]

*The Effects of Cold Exposure on Wet Aircraft Passengers: A Review.* Garner, Robert P.; Wilcox, Bruce C.; England, Harvey M.; Nakagawara, Van B. Report No. DOT/FAA/AM-94/10. A special report prepared for the U.S. Federal Aviation Administration (FAA) Office of Aviation Medicine. May 1994. 16 p.; ill.; appendices. Available through U.S. National Technical Information Service (NTIS)*.

Keywords

1. Aviation

2. Thermoregulation

3. Hypothermia

Summary: Cabin water spray systems (CWSS) aboard commercial passenger aircraft have been suggested as a method of reducing passenger death and injury from fire and smoke, often associated with aircraft accidents. The report examined physiological responses of people who were exposed to the elements after being saturated with moisture from a CWSS. The report said that the severity of the exposure would be proportional to wind speed and to the degree to which the individual was doused, and inversely proportional to ambient temperature. The authors said that experiments to develop models to predict the severity of cold injury under variable environmental and wetness conditions still need to be designed. A full investigation would be better able to determine if the survival benefits of a CWSS outweigh the health risks, the authors said. [from abstract]

*Unreported Medications Used in Incapacitating Medical Conditions Found in Fatal Civil Aviation Accidents.* Canfield, Dennis V.; Flemig, Jo; Hordinsky, Jerry; Veronneau, Stephen. Report No. DOT/FAA/AM-94/14. A special report prepared for the U.S. Federal Aviation Administration (FAA) Office of Aviation Medicine. August 1994. 8 p.; ill. Available through U.S. National Technical Information Service (NTIS)*.

Keywords

1. Medical Conditions — Unreported — Drugs — Aviation

Summary: The FAA Civil Aeromedical Institute's (CAMI's) Toxicology and Accident Research Laboratory analyzes all fatal aviation accidents that occur in the United States. Between 1987 and 1992, the Toxicology and Accident Research Laboratory received specimens from 2,192 pilots for post-mortem toxicology analysis. Drugs used to treat potentially incapacitating medical conditions were found in 48 of the cases: 13 cardiovascular, 28 psychiatric and seven neurological. In most of cases, the drugs or illnesses would have caused the Office of Aviation Medicine to reject the pilot's certification. [from abstract]

## Books

*ATP, Airline Transport Pilot: A Comprehensive Text and Workbook for the ATP Written Exam, fourth edition.* Boyd, K.T. Ames, Iowa, U.S.: Iowa State University Press, 1994. 174 p.; index; appendices.

Keywords

1. Aeronautics — Examinations, questions, etc.

2. Airplanes — Piloting — Examinations, questions, etc.

3. Air pilots — Licenses — United States

4. Transport planes — Examinations, questions, etc.

Summary: The book leads the reader logically through the steps and knowledge necessary to carry out a flight under U.S. Federal Aviation Regulations (FARs) Part 121. Chapters cover computer functions and problems, weight and balance, preflight regulations, flight planning, navigational aids (NAVAIDS), en route regulations, meteorology, weather reports and depictions, and terminal procedures and regulations. Each chapter ends with a quiz, and a sample Airline Transport Pilot (ATP) examination is included. Answers for all tests in the book are supplied.

*Aviation Psychology in Practice.* Johnston, Neil; McDonald, Nick; Fuller, Ray, eds. Brookfield, Vermont, U.S.: Ashgate Publishing Co., 1994. 390 p.; ill.; index. ISBN 0-291-39808-1.

Keywords

1. Aeronautics — Psychology

2. Psychology, Industrial

3. Aeronautics, Commercial — Safety measures

4. Aeronautics — Human factors

Summary: The book, published in conjunction with the 21st Conference of the Western European Association for Aviation Psychology, Dublin, Ireland, March 1994, seeks to broaden the focus of aviation psychology beyond the flight deck to include the entire aviation system. It also discusses new theoretical developments that are shaping aviation psychology. The 15 essays in the book are contained in four sections: "The Aviation Socio-technical System," "Learning from Accidents and Incidents," "New Theoretical Models" and "The Delivery of Training." The book and the conference were activities of the Aerospace Psychology Research Group of Trinity College, Dublin. Contributors include Earl L. Wiener, R. Curtis Graeber and Helen C. Muir. ♦

* U.S. Department of Commerce
National Technical Information Service
Springfield, VA 22161 U.S.
Telephone: 703-487-4780

## Updated U.S. Federal Aviation Administration Reference Materials

**Advisory Circulars (ACs)**

| AC Number | Date | Subject |
|---|---|---|
| AC 150/5200-28A | 8/10/94 | Change 1 to *Notices to Airmen (NOTAMs) for Airport Operators* |
| AC 00-44FF | July 1994 | *Status of Federal Aviation Regulations*. Cancels AC 00-44EE |
| 150/5370-10A | 7/6/94 | Change 8 to *Standards for Specifying Construction of Airports* (Revises Item F-162, Chain Link Fences) |
| 150/5370-10A | 5/20/94 | Change 7 to *Standards for Specifying Construction of Airports* |
| AC 150/5220-20 | 3/1/94 | Change 1 to *Airport Snow and Ice Control Equipment, Chg 1* (cancels AC 150/5220-12, dated June 12, 1978) |
| AC 150/5360-13 | 1/19/94 | Change 1 to *Planning and Design Guidelines for Airport Terminal Facilities* |
| AC 23-14 | 9/30/93 | *Type Certification Basis for Conversion from Reciprocating Engine to Turbine Engine-powered Part 23 Airplanes* |

**U.S. Federal Aviation Regulations (FARs)**

| Part | Date | Subject |
|---|---|---|
| Part 135 | 6/21/94–7/29/94 | Air Taxi Operators and Commercial Operators (Change 3, incorporating Amendment 135–49, Emergency Locator Transmitters, adopted June 10, 1994, which affects §135.167(c); and Amendment 135–50, Exit Seating for On-demand Operations, adopted June 21, 1994, which affects §135.129). |

# Blankets in Overhead Bin Appear to Have Been Deliberately Ignited

***The NTSB recommended that the FAA establish a flammability test method and performance standard for blankets supplied to airlines.***

*Editorial Staff*

*The following information provides an awareness of problems through which such occurrences may be prevented in the future. Accident/incident briefs are based on preliminary information from government agencies, aviation organizations, press information and other sources. This information may not be entirely accurate.*

Air Carrier

## Fire in Overhead Bin Prompts Safety Recommendations

*Boeing 727-251. Minor damage. Two minor injuries.*

The aircraft was being pushed back from the gate in Montreal, Canada, when smoke was detected in an overhead storage compartment in the passenger cabin.

Crew members quickly extinguished the fire with two Halon fire extinguishers. Two passengers were injured in the emergency evacuation and the aircraft suffered minor heat and smoke damage.

The incident was investigated by the Transportation Safety Board of Canada (TSB) and the U.S. National Transportation Safety Board (NTSB). The investigation determined that the fire originated in several blankets stored in the overhead bin, but no ignition sources were found in the compartment or in a carry-on bag stowed there. The incident report said that on the day after the fire, investigators found a fire-scorched paper towel in each of the two aft lavatories and a burned match beside each towel. "The evidence strongly suggested that the fire in the overhead compartment had been deliberately set," the incident report said.

The report said that blankets identical to those stored in the overhead bins were examined following the fire. "The fabric, 100-percent polyester, ignited easily with a match," the report said. "Following ignition, the polyester melted and resulted in a molten polyester fire."

The NTSB concluded that "allowing the use of highly flammable blankets for passenger comfort is inconsistent with current FAA [U.S. Federal Aviation Administration] standards and requirements to reduce the flammability of interior cabin materials" and recommended that the FAA develop a "fire performance test method and performance criteria (standard) for blankets supplied to commercial operators." The NTSB added that operators should then be required to use only blankets that meet those standards.

## Side-step Maneuver Ends on Wrong Runway

*Boeing 737-300. No damage. No injuries.*

During an instrument landing system (ILS) approach on Runway 17L, the crew of the Boeing 737 was advised by air traffic control (ATC) to expect a visual side-step to Runway 17R and to report when the runway was in sight.

When the crew reported the runway in sight, ATC cleared the aircraft to land on 17R. Weather at the time was reported as scattered clouds at 800, 3,000 and 14,000 feet (244, 914 and 4,267 meters), ceiling 20,000 feet (6,096 meters) broken with light rain.

Just before executing the side-step, the crew identified what they believed was 17R, based on runway light intensity and a landing aircraft ahead of them. The landing aircraft ahead of the B-737 was actually a commuter landing on Runway 18. The controller, unsure of the B-737's location after its landing, directed the next aircraft in sequence to go around. Once the B-737 was established on the approach to the wrong runway, its descent rates also met criteria for an unstabilized approach.

The crew did not realize that they had landed on the wrong runway until they noticed that signage and taxiway geometry did not match what they had expected to see.

Air Taxi
Commuter

## Improper STOL Procedures Stall Commuter

*De Havilland DHC-6. Substantial Damage. One serious injury. One minor injury.*

The DHC-6 Twin Otter became airborne after a take-off roll of about 300 feet. The aircraft initially began to climb, but then started to descend. The aircraft then climbed again, more steeply than before, then suddenly descended again in a steep nose-down attitude, crashing halfway down the runway.

No passengers were on board. The captain sustained minor injuries and the first officer was seriously injured.

An investigation conducted by the Transportation Safety Board of Canada (TSB) determined that inappropriate short-takeoff and landing (STOL) procedures had been applied by the crew.

The TSB said that Transport Canada (TC), using information from the TSB accident investigation, "advised its regional offices that all Twin Otter operators should be made aware that STOL operations outlined in the Supplemental Operating Procedures [in aircraft flight manuals] are not authorized in commercial operations."

The TSB added: "Most aircraft flight manuals contain two types of information. One type is approved and mandatory information on the operation of the aircraft. The other, non-approved, includes supplemental operating procedures from the aircraft manufacturer that have not necessarily been reviewed by the certificating authorities and thus might not meet safety margins expected for commercial usage of the aircraft."

The TSB noted that the Twin Otter "has an international reputation as a STOL aircraft and is often utilized in operations demanding short field operations. However, in the flight manual for this aircraft, warning sections indicating that the maximum performance STOL configuration does not meet certification standards are not prominently displayed, nor are the operating limitations generally understood by operators of the Twin Otter."

The TSB recommended that the Canadian Department of Transport "define, through a program of flight testing, the aircraft configuration and operating conditions under which 'maximum performance' STOL takeoffs are authorized" and advise all DHC-6 operators "on a global basis of the operating limitations" for these STOL procedures.

Corporate
Executive

## Hypoxia Blamed for Fatal Crash

*Cessna 340. Aircraft destroyed. One fatality.*

The twin-engine Cessna was on a night ferry flight cruising at 25,000 feet (7,620 meters). During the flight, the pilot left the cockpit to use the lavatory located in the rear of the aircraft.

Although oxygen was available in the cockpit, supplemental oxygen was not available in the cabin. The aircraft crashed three hours and 57 minutes after departure. The pilot's body was found in the aft cabin area.

A subsequent investigation revealed that the aircraft had been operated with a known pressurization system deficiency that limited the aircraft to 17,000 feet (5,182 meters) mean sea level while maintaining a cabin altitude of 10,000 feet (3,048 meters). It was determined that the left engine failed because of fuel starvation. Propeller signatures indicated that the right engine was developing power at impact. The investigation concluded that the pilot suffered from hypoxia and was unable to return to the cockpit.

## Pilot Killed on Familiarization Flight; Lack of Systems Knowledge Cited

*Cessna 421. Aircraft destroyed. One fatality.*

During a familiarization flight by the newly hired commercial pilot, the right engine failed because of fuel starvation. The aircraft crashed in a pasture in a nose-down, left-wing-low vertical descent angle. A post-impact fire consumed the cabin and left wing.

An investigation determined that neither propeller was feathered and that the landing gear was in the extended-and-locked position. Flaps had also been lowered to a 45-degree position.

The pilot had not been checked in the aircraft and was not familiar with the operation of the fuel system or emergency procedures for the aircraft, investigators said. The airspeed decreased below the minimum controllable airspeed and the aircraft stalled.

# Other General Aviation

## Engine Failure Mars Training Flight

*Cessna 172. Substantial damage. Two minor injuries.*

The student was practicing pattern work with an instructor. When the aircraft was at 600 feet (183 meters), the instructor reduced engine power to idle to simulate an engine failure. At 300 feet (91 meters), the throttle was advanced but the engine did not respond. An off-airport landing was made on a field. During the landing roll, the instructor ground looped the aircraft to avoid a ditch at the end of the field. The aircraft came to rest inverted and the student and instructor received minor injuries.

## Heavy Landing Sends Aircraft Off Runway

*Piper PA-28. Substantial damage. No injuries.*

The single-engine Piper was attempting to land on Runway 25 after a short cross-country flight. When the aircraft was about 15 feet (5 meters) off the ground, at 85 knots, the wind diminished and the aircraft dropped heavily onto the runway.

The nose wheel collapsed, the propeller struck the runway and the aircraft veered off the runway into the grass. As the aircraft departed the runway, the right main gear collapsed and the right wing was damaged. Surface winds at the time were reported as 320 degrees at 10 knots.

# Rotorcraft

## Water in Fuel Tank Cuts Flight Short

*Schweizer 300C. Substantial damage. One serious injury.*

The Schweizer was on an aerial observation mission when it experienced a loss of engine power after take off at about 300 feet (91 meters) above ground level. The pilot entered autorotation and the helicopter collided with the ground.

During a post-crash examination, about one and one half gallons of water was recovered from the right main fuel tank. The pilot was seriously injured and the helicopter sustained substantial damage in the accident. Weather at the time was reported as clear skies, visibility 15 miles (24 kilometers) and winds at 5 knots. ♦

BLANK
INSIDE
BACK
COVER

**FLIGHT SAFETY DIGEST**

Staff: Roger Rozelle, director of publications; Girard Steichen, assistant director of publications; Kate Achelpohl, editorial assistant; Rick Darby, editorial consultant; and Dwyane D. Feaster, production consultant.

Subscriptions: US$95 (U.S.-Canada-Mexico), US$100 Air Mail (all other countries), twelve issues yearly. • Include old and new addresses when requesting address change. • Flight Safety Foundation, 2200 Wilson Boulevard, Suite 500, Arlington, VA 22201-3306 U.S. • telephone: (703) 522-8300 • telex: 901176 FSF INC AGTN • fax: (703) 525-6047

## We Encourage Reprints

Articles in this publication may be reprinted in whole or in part, but credit must be given to: Flight Safety Foundation, *Flight Safety Digest*, the specific article and the author. Please send two copies of reprinted material to the director of publications.

## What's Your Input?

In keeping with FSF's independent and nonpartisan mission to disseminate objective safety information, Foundation publications solicit credible contributions that foster thought-provoking discussion of aviation safety issues. If you have an article proposal, a completed manuscript or a technical paper that may be appropriate for *Flight Safety Digest*, please contact the director of publications. Reasonable care will be taken in handling a manuscript, but Flight Safety Foundation assumes no responsibility for material submitted. The publications staff reserves the right to edit all published submissions. Payment is made to author upon publication. Contact the Publications Department for more information.